

UNIVERSIDADE FEDERAL DO RIO GRANDE DO SUL

INSTITUTO DE BIOCÊNCIAS

BACHARELADO EM BIOTECNOLOGIA

TRABALHO DE CONCLUSÃO DE CURSO

BEN HUR NEVES DE OLIVEIRA

CARACTERIZAÇÃO *IN SILICO* DO MODELO DE INTERAÇÃO DE
GENES DA AUTO-RENOVAÇÃO DAS CÉLULAS TRONCO E
SINALIZAÇÃO POR CÁLCIO EM METÁSTASES DE MELANOMA
HUMANO

Porto Alegre

2016

BEN HUR NEVES DE OLIVEIRA

Caracterização *in silico* do Modelo de Interação de Genes da Auto-Renovação
das Células Tronco e Sinalização por Cálcio em Metástases de Melanoma
Humano

Trabalho de Conclusão de Curso
submetido à Universidade Federal
do Rio Grande do Sul como parte
dos requisitos necessários para
obtenção do Grau de Bacharel em
Biotecnologia.

Orientadora: Prof.^a Dr.^a Carla Dalmaz

Co-orientador: Dr. Fares Zeidán Chuliá

AGRADECIMENTOS

Meus votos de gratidão vão:

Em primeiro lugar, aos meus pais, por toda paciência ofertada no período dessa minha longa e torta jornada acadêmica. Meus pais são os pilares da minha fortaleza, meus modelos de vida, minhas fontes de amor eterno. Estendo esses votos ainda aos meus irmãos, sobrinhos e cunhado, os quais completam minha família e fazem com que eu me sinta uma pessoa de sorte.

A ambos os meus orientadores: prof^a Carla e, em especial, meu co-orientador, dr. Fares, com quem venho trabalhando desde o início da minha graduação e com quem desenvolvi um laço de amizade. O dr. Fares foi (e continua sendo) um grande mestre para mim, com quem aprendi lições valiosas sobre o fazer científico e a busca pelo conhecimento.

Aos meus melhores amigos, com quem convivo há mais de uma década. Nos momentos de alegrias, celebrações ou vitórias, eles estiveram ao meu lado. Nos momentos de tristezas, frustrações ou derrotas, eles estiveram ao meu lado. Esse é o único jeito que sei para se reconhecer amizades verdadeiras. *"I get by with a little help from my friends"...*

Aos professores Janette Palma Fett e Artur Germano Fett Neto, que gentilmente abriram as portas de seus laboratórios para mim nesse último semestre de graduação para a realização do meu estágio obrigatório curricular, uma experiência que definitivamente expandiu meus horizontes no meio acadêmico e, por isso, sou muito grato.

Por fim, aos colegas do Laboratório de Fisiologia Vegetal, que me acolheram muito bem e fizeram com que eu me sentisse em casa. Em especial, ao Artur Júnior e Janete Adamski, com quem trabalhei de perto e sempre me ajudaram com muita paciência.

RESUMO

Melanoma é um câncer de pele muito suscetível à ocorrência de metástases e, por isso, é considerado uma neoplasia maligna agressiva. Até hoje, mais de 90% das causas de morte por câncer são atribuídas à ocorrência de metástases. Acredita-se, ainda, que especificamente um subconjunto de células da população de um tecido tumoral é capaz de semear e repopular o seu tumor de origem. Estudos evidenciam que essas células “iniciadoras” de tumores comumente possuem características semelhantes às de células tronco, tais como poder de auto-renovação e capacidade de dar origem a células progenitoras ou diferenciadas, o que lhes rendeu o nome de células tronco tumorais (CTTs). Existem evidências de que a via de sinalização do íon cálcio tem papel fundamental em uma série ampla de processos biológicos, dentre os quais estão o comprometimento celular na diferenciação de células tronco. Sendo assim, nós questionamos no presente estudo a influência da via de sinalização do Ca^{2+} na regulação da pluripotência de células tronco dentro de um contexto de neoplasia maligna. Para isso, nós criamos uma rede *in silico* (“STEMCa”) de interação proteína-proteína para modelar a integração de ambas as vias (sinalização por Ca^{2+} e regulação de pluripotência de células tronco). Após, nós avaliamos a expressão dos genes que codificam as proteínas desse modelo, utilizando um repositório público de microarranjos. Para os dados de expressão, foram utilizadas apenas amostras clínicas de melanomas metastáticos (tendo tumores primários como controle) de três conjuntos independentes de amostras de pacientes. Por fim, utilizamos ferramentas de biologia de sistemas para inferir potenciais candidatos a alvos terapêuticos e/ou marcadores de metástase. Nossa análise de expressão diferencial indica que, em ao menos um dos conjuntos de amostras de pacientes, 51% dos genes do modelo construído (151 de um total de 294 genes) encontram-se consistentemente desregulados (valor de p corrigido <0.05) em metástases de melanoma quando são comparados com amostras de tumor primário, sugerindo que, de fato, as vias avaliadas têm expressão aberrante. Além disso, nossos cálculos topológicos em cima do modelo proposto apontam *GNAQ*, *GSK3B*, *GSTP1*, *MAPK3*, *PPP1CC*, *PRKACA*, e *SMAD4* como potenciais candidatos a serem estudados para intervenções terapêuticas ou como biomarcadores.

Palavras-chave: célula tronco tumoral; metástase; cálcio; pluripotência; biologia de sistemas.

ABSTRACT

Melanoma is a skin cancer with high incidence to develop metastasis and, therefore, it is considered to be an aggressive malignant neoplasm. To date, more than 90% of cancer-related causes of death are still attributed to the occurrence of metastasis. It has been postulated that a subset of cells within the tumor tissue is solely capable of seeding and restore the whole tumoral tissue. A number of studies have reported that these tumor-initiating cells also named as *cancer stem cells* (CSCs) commonly display stem-like properties, such as self-renewal and also potency (*i.e.* they are able to give rise to progenitor or differentiated cells). Calcium ion (Ca^{2+}) signaling pathway plays a fundamental role on a broad series of biological processes, and its role in stem cell fate and commitment to differentiation has additionally been proposed. Hence, one could speculate whether Ca^{2+} signaling pathway and stem cell pluripotency regulation crosstalk may influence the metastatic transformation of melanoma cancer cells. In order to find evidence for this role, we build an *in silico* protein-protein interaction network (“STEMCa”) to model the integration of both pathways (Ca^{2+} signaling and stem cell pluripotency regulation). Thereafter, we evaluated the expression pattern of the genes coding for the proteins within the “STEMCa” model by utilizing three publicly available microarray datasets from human patients found in Gene Expression Omnibus (GEO). For our analysis, we compared data from clinical samples of melanomas metastasis with primary tumors (controls). Finally, we used systems biology tools to identify putative therapeutic targets *in silico* and/or candidate biomarkers for melanoma metastasis. Our analysis revealed that the expression profile of the genes within our “STEMCa” model is consistently deregulated, with 151 out of 294 of its members (51%) displaying significant changes of expression (corrected p -value <0.05) in at least one of the datasets of melanoma metastases, when compared with primary biopsy tumors. This suggests that the integrated pathways comprising our network are aberrant in gene expression. In addition, topological measurements of “STEMCa” model point towards *GNAQ*, *GSK3B*, *GSTP1*, *MAPK3*, *PPP1CC*, *PRKACA*, and *SMAD4* as optimal candidates *in silico* to be further studied as potentially good therapeutic targets or biomarkers.

Key words: cancer stem cell; metastasis. calcium; pluripotency; systems biology

SUMÁRIO

1. Introdução.....	6
2. Manuscrito do Artigo.....	11
3. Discussão dos Resultados.....	51
4. Referências Bibliográficas.....	56

1. Introdução

Fundamentalmente todo organismo multicelular origina-se de uma única célula com o potencial de dar origem a todas as linhagens celulares que compõe os seus tecidos (Dreesen e Brivanlou, 2007). Tal célula deverá apresentar duas propriedades básicas, as quais os biólogos denominam:

- Auto-renovação: por divisão celular assimétrica, uma célula tronco (CT) divide-se em duas células, de maneira que uma das células é idêntica a célula mãe (*i.e.* com as mesmas propriedades de uma CT), e a outra compromete-se com algum destino celular e detendo algum grau menor de características de CT.
- Potência: é a capacidade que uma célula possui de dar origem às novas linhagens celulares. Em humanos, por exemplo, faz-se a seguinte classificação: a célula é totipotente se for capaz de originar todos os tipos celulares do organismo; pluripotente se for capaz de originar qualquer célula das três camadas germinativas (mas não do trofoblasto extraembrionário) ou, por fim, multipotente se for capaz de dar origem a um conjunto restrito de células tecido-específicas dentro de uma única camada germinativa. Nessa classificação, ainda podemos citar as células oligopotentes (capazes de dar origem a um conjunto mais restrito ainda de tipos celulares em comparação às multipotentes) e também as unipotentes (capazes de gerar apenas células do próprio tipo).

Embora o papel das células tronco (CTs) seja evidente no desenvolvimento embrionário, os tecidos adultos mantêm uma pequena subpopulação de CTs adultas que mantêm as propriedades de auto-renovação e pluri ou multipotência, com a finalidade de manter e reaver a homeostase dos tecidos em caso de lesões (Brack e Rando, 2012).

Conceitualmente, células tronco tumorais (CTTs) possuem características semelhantes às de CTs, tais como poder de auto-renovação e capacidade de diferenciarem-se em novos tipos celulares, porém apresentam perda do controle do ciclo celular (característica tumoral) (Allan *et al.*, 2006). Devido a tais características, discute-se, nas últimas décadas, a hipótese de que na heterogênea população tumoral existe uma pequena subpopulação de CTTs que são capazes de sozinhas semear a tumorigênese. De fato, já em 1937, Furth *et al.*

reportaram que apenas uma pequena porção de células era capaz de induzir tumorigênese em camundongos após esses animais terem recebido injeção subcutânea de poucas células oriundas de um tumor leucêmico (Furth e Kahn, 1937). Contudo, foi apenas em meados dos anos 90 que a hipótese das CTTs como semente dos tumores ganhou força, especialmente através dos trabalhos de Dick *et al.*. Esses autores separaram células CD34⁺/CD38⁻ (raras na população heterogênea do tumor) de leucemia aguda mielóide e as transplantaram para camundongos imunodeficientes, resultando na mesma doença e com características semelhantes às do tumor que a originou, ao passo que outras células testadas não apresentaram este desfecho (Lapidot *et al.*, 1994). Ou seja, supostamente um pequeno subconjunto de toda população tumoral é suficiente para repopular todo o tumor de origem. Vale ressaltar, sobretudo, que CTTs já foram também identificadas em tumores sólidos, tais como câncer de mama (Al-Hajj *et al.*, 2003), cérebro (Singh, Hawkins, *et al.*, 2004), pulmão (Eramo *et al.*, 2008) e pele (Schatton *et al.*, 2008).

Acredita-se que as CTTs podem se originar de CTs adultas normais por aquisição de mutações em oncogenes, fazendo com que a célula mutada perca o controle da regulação do ciclo celular e passe a dividir-se de maneira aberrante (Li *et al.*, 2007). De fato, muitas proteínas de superfície marcadoras de CTs adultas são também encontradas em CTTs, sugerindo uma relação de origem entre ambas. Outra hipótese é a de que as CTTs originam-se de células tumorais diferenciadas, mas que adquiriram mutações que induziram-nas a um processo de desdiferenciação, fazendo-as adquirir características de CTs (Li *et al.*, 2007). Sabe-se que esse tipo de reprogramação celular é factível, pois já foi demonstrado que é possível transformar fibroblastos humanos em células pluripotentes através da indução da expressão ectópica de alguns fatores de transcrição nessas células (Park *et al.*, 2008). No entanto, a regulação das vias que controlam essa reprogramação celular *in vivo* são muito complexas, de maneira que torna-se conceitualmente difícil dar crédito ao surgimento espontâneo de CTTs a partir de células diferenciadas. Por outro lado, tendo em vista que a proporção de CTs para as demais células de um tecido qualquer é extremamente baixa, isso torna a ideia do acúmulo de mutações em CTs também um cenário improvável. Todavia é importante lembrar que o estado de diferenciação celular não é uma propriedade discreta, portanto existe uma gradiente de células com fenótipos intermediários em abundância relativa nos tecidos. Além disso, nenhuma dessas hipóteses é mutuamente exclusiva, de maneira que é possível que ocorram concomitantemente.

As CTTs já foram também implicadas na recorrência de tumores pós-tratamento, devido sua característica intrínseca de resistência aos quimioterápicos, os quais tem como estratégia terapêutica clássica a indução da morte celular por apoptose (Zhao, 2016). As próprias CTs normais já apresentam altos níveis de expressão de genes relacionados à sobrevivência e anti-apoptóticos, ou seja, possivelmente as CTTs contem com sistemas de proteção pré-existentes (He *et al.*, 2014). Além disso, a superexpressão de bombas de efluxo multidrogas ATP-dependentes já foi reportada para CTTs de vários tumores, o que demonstrou-se apresentar alta correlação com os níveis de reincidência de câncer (Koren e Fuchs, 2016). Vale ressaltar ainda que as CTTs comumente apresentam altos níveis de expressão de aldeído-desidrogenase (ALDH), o que também tem sido correlacionado ao poder de invasividade e quimioresistência (Crocker *et al.*, 2009). Por exemplo, Chafaret-Jauffret *et al* demonstraram que células ALDH⁺ isoladas de câncer de mama são mais invasivas que as ALDH⁻ (Charafe-Jauffret *et al.*, 2010). E, ainda em câncer de mama, Kai *et al* apontam que encontra-se preferencialmente uma subpopulação CD44⁺/CD24⁻ (marcador tronco) em tecidos metastáticos oriundos de amostras clínicas (Kai *et al.*, 2011).

Outro evento molecular que tem sido vinculado a metástases em alguns tipos de câncer é a presença de oscilações intracelulares de cálcio (e.g., câncer de mama e de próstata) (Rizaner *et al.*, 2016). Em geral, O íon cálcio (Ca²⁺) tem papel importante nos sistemas biológicos por suas propriedades químicas intrínsecas, sendo este um íon divalente com mais afinidade a átomos de oxigênio (O) do que nitrogênio (N) ou enxofre (S) (Carafoli e Krebs, 2016). Além disso, o Ca²⁺ é capaz de ligar-se a todos os átomos de O de grupamentos carboxilados de biomoléculas. Tais propriedades marcam esse íon como uma espécie bastante reativa em sistemas biológicos, e os organismos evoluíram de modo a utilizá-lo como agente sinalizador, provavelmente pela elevada exposição ao mineral cálcio (abundante na crosta terrestre). Por outro lado, essa alta reatividade implicou também a evolução de mecanismos para controlar a concentração intracelular de Ca²⁺, tais como:

- Compartimentalização: o Ca²⁺ é depositado e mantido em diferentes subcompartimentos celulares.
- Externalização/Internalização: o Ca²⁺ pode ser bombeado através das membranas dos subcompartimentos celulares quando necessário.
- Quelação: biomoléculas ligam-se estavelmente ao Ca²⁺, aprisionando-o e impedindo que se ligue a outras moléculas.

A ligação do Ca^{2+} a biomoléculas pode tanto ativá-las quanto reprimí-las, pois as interações eletrostáticas induzem alterações conformacionais nas proteínas, alterando sua estrutura tridimensional e, portanto, sua funcionalidade. Em geral, a sinalização por cálcio refere-se a um sinal induzido ou transduzido pelo Ca^{2+} por meio da elevação de sua concentração intracelular, disparando uma série de reações e, por fim, re-estabilizando os níveis de Ca^{2+} no estado basal. A dinâmica do sinal é tal que o Ca^{2+} é sequestrado e trocado entre subcompartimentos, aqui incluídos citosol, mitocôndria, retículo endoplasmático, cisternas trans do complexo de Golgi e núcleo (Berridge *et al.*, 2003). A sinalização por Ca^{2+} tem papel fundamental em diversos processos biológicos, tais como excitabilidade, exocitose, mobilidade, apoptose, transcrição e diferenciação — para citar alguns (Clapham, 2007). O que distingue um sinal de outro é essencialmente a amplitude e a frequência de variação da concentração intracelular de Ca^{2+} , além da natureza do próprio estímulo. Sendo assim, as oscilações de $[\text{Ca}^{2+}]$ na célula são finamente reguladas por uma maquinaria celular que, quando corrompida, pode levar a uma série de patologias, incluindo a transformação, promoção e progressão de câncer (Tsai *et al.*, 2015).

De entre todos os tipos de câncer, o melanoma é um dos mais suscetíveis ao desenvolvimento de metástases e, portanto, muito agressivo. Segundo estimativas do Instituto Nacional do Câncer (INCA), o melanoma representa, no Brasil, cerca de 3% das neoplasias malignas. Embora a incidência seja baixa, a letalidade desse tipo de câncer é bastante elevada e suas chances de cura são baseadas principalmente na detecção precoce do tumor. Alguns marcadores correlacionados a CTTs já foram associados ao poder metastático de melanomas, tais como CD20, CD133, CD271 (três proteínas de superfície), ABCB5 (membro da família das bombas de efluxo ATP-dependentes) e ALDH1A (uma isoforma da ALDH) (Kozovska *et al.*, 2016). Com referencia ao cálcio, tem sido recentemente descrito a super-expressão de canais de cálcio tipo T em melanoma humano sendo estes vinculados à proliferação celular (Maiques *et al.*, 2016). Além disso, a concentração de cálcio no soro humano correlaciona com o estágio do melanoma cutâneo, sendo este sugerido como marcador da progressão do câncer (Datta *et al.*, 2016). Contudo, o papel do cálcio e de moléculas dependentes da sinalização por cálcio no processo de metástases é pouco compreendido e tem sido muito menos estudado.

No intuito de conectar esse aparato de informações, surge o interesse em se estudar o papel da integração das vias de sinalização do Ca^{2+} concomitantemente à regulação da pluripotência de CTs no contexto de metástase em melanomas humanos. Para atingir o

objetivo de se estudar vias tão complexas simultaneamente e de maneira eficaz, torna-se indispensável a utilização de métodos computacionais. A Biologia de Sistemas é uma área da Bioinformática que aborda a modelagem de redes de interação entre biomoléculas e/ou metabólitos e compostos através de grafos. Na matemática, a Teoria de Grafos vem sendo desenvolvida desde o século XVIII, e atualmente são muitos os métodos para se analisar suas propriedades (mesmo para grafos de elevada complexidade). Sendo assim, pesquisadores vêm usufruindo desses métodos para melhor entender o perfil do funcionamento modular das redes proteicas em células, haja visto que um organismo vivo opera sob influência conjunta de milhares de biomoléculas interagindo entre si. Atualmente, são muitos os bancos de dados com coleções de anotações para todo tipo de informação biológica (seja para genômica, proteômica, metabolômica, interatômica etc), viabilizando o processo de modelagem de sistemas biológicos. No estudo a seguir, montamos uma rede de interações proteína-proteína, integrando as vias de sinalização do cálcio e regulação da pluripotência de células tronco, e avaliamos a dinâmica de expressão dos genes que codificam essas proteínas em diferentes amostras primárias de melanomas humanos, comparando o perfil de expressão de tumores primários e metastáticos.

2. Manuscrito do artigo a ser submetido à revista *Cell Calcium*

(ISSN: 0143-4160; Impact Factor: 2.909)

Network-based Identification of Altered Stem Cell Pluripotency and Calcium Signaling Pathways in Metastatic Melanomas

Ben-Hur Neves de Oliveira, Carla Dalmaz¹ & Fares Zeidán-Chuliá^{1,2*}

¹*Programa de Pós-Graduação em Ciências Biológicas: Bioquímica, Departamento de Bioquímica, Instituto de Ciências Básicas da Saúde, Universidade Federal do Rio Grande do Sul (UFRGS), Porto Alegre, RS, Brazil;* ²*Faculty of Medicine, University of Turku, Turku, Finland.*

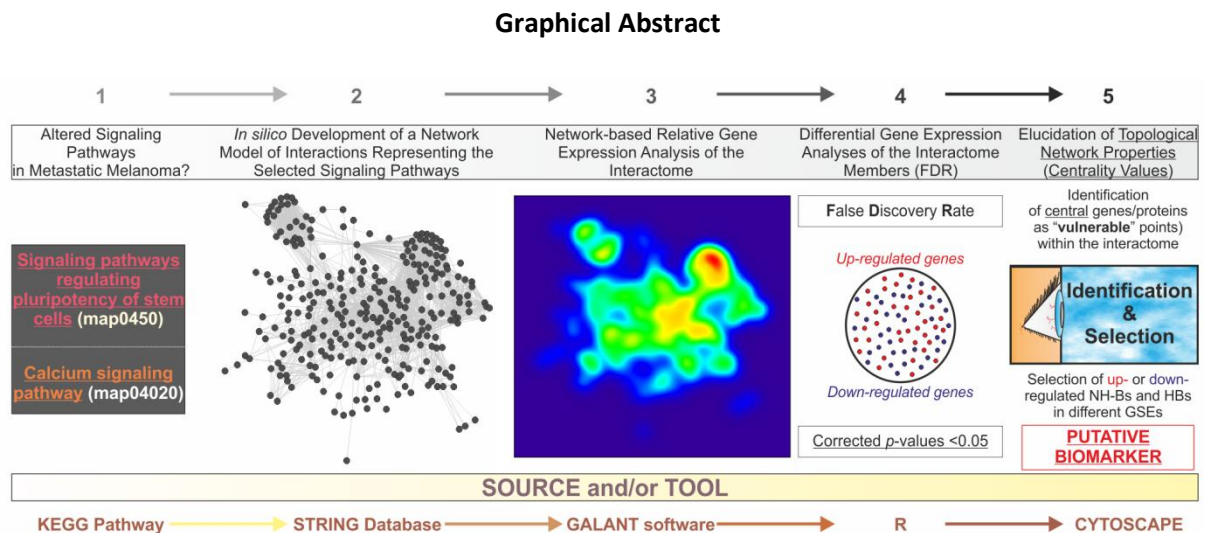
Running title: Aberrant stem cell-Ca²⁺ signaling network in melanoma metastases.

Abbreviations: CSC, cancer stem cell; CON, connector; FDR, false discovery rate; HB, hub- bottleneck; NH-B, non-hub-bottleneck; PPI, protein-protein interaction; SC, stem cell.

ABSTRACT

Malignancy of cancer has been linked to distinct subsets of stem-like cells, the so-called “cancer stem cells” (CSCs) which persist during treatment and seems to lead to drug-resistant recurrence. Metastatic spread of cancer cells is one of the hallmarks of malignancy and contributes to the majority of human melanoma-related deaths. Overlapping groups of proteins and pathways have recently been identified to regulate both stem cell migration and cancer metastasis, raising the question whether genes/proteins involved in stem cell pluripotency may have important implications when applied to the biology of cancer metastasis. Furthermore, it is well known that ion channels and receptors, particularly those responsible for calcium (Ca^{2+}) signal generation, are critical in determining the cellular fate of stem cells (SCs). In the present study, we searched for evidence for altered stem cell pluripotency and Ca^{2+} signaling-related genes in the context of melanoma metastases when compared to primary tumors, by network analysis of gene expression of biopsy tissue from three different datasets of patients. We created an *in silico* network model (“STEMCa” interactome) showing the landscape of interactions between stem cell pluripotency and Ca^{2+} signaling-related genes/proteins and demonstrated that around 51% (151 out of 294) of the genes within this model displayed significant changes of expression (FDR, corrected p -value <0.05) in at least one of the datasets of melanoma metastases when compared with primary biopsy tumors. Analysis of the topological network properties (*degree* and *betweenness*) revealed 27 members as the most central hub- (HB) and non-hub-bottlenecks (NH-B) among the 294 genes/proteins of the whole interactome. From those representative genes, *CTNNB1*, *GNAQ*, *GSK3B*, *GSTP1*, *MAPK3*, *PPP1CC*, *PRKACA*, and *SMAD4* showed equal up- or down-regulation (corrected p -value <0.05) in at least 2 datasets of melanoma metastases samples and only *PTPN11* showed up-regulation (corrected p -value <0.05) in the three of them, when compared with primary tumor samples. We postulate that altered expression of stem cell pluripotency and Ca^{2+} signaling pathways-related genes may contribute to the metastatic transformation, being these central members an optimal candidate group of biomarkers and *in silico* therapeutic targets for melanoma metastasis.

Keywords: pluripotency; stemness; calcium; malignancy; biomarker; systems biology.



Description. General abstract workflow summarizing the criteria and tools utilized for the present study. Two maps from the KEGG PATHWAY Database corresponding to "Signaling pathways regulating pluripotency of stem cells" (map0450) and "Ca²⁺ signaling pathway" (map04020) were selected. Thereafter, an interactome was developed for integrating these maps into one single gene/protein interaction network model by the STRING V10.0 database (<http://string-db.org/>). With GALANT, we projected numerical data from three different datasets extracted from GEO database (<http://www.ncbi.nlm.nih.gov/geo/>). The 2D views correspond to the relative gene expression onto the newly-developed interactome. This tool creates three smoothed data plots that resemble the network model layout. Differential gene expression analysis was performed by using the R environment (*limma* package). The *p*-values were adjusted for multiple comparisons by calculating false discovery rates (FDR), in order to avoid potential false positives. By using Cytoscape, further identification of "vulnerable" points within the *in silico* model upon elucidation of centrality values and selection of those central (NH-Bs and HBs) up- or down-regulated genes, suggest candidate diagnostic biomarkers and also potential molecular targets for therapeutics.

1. Introduction

During the last 20 years of cancer research, the arise of the so-called cancer stem cell (CSC) theory still generates controversies among the scientific community as critical players in tumorigenesis, with the main characteristics of (i) initiate, (ii) maintain, (iii) re-grow diverse tumors and (iv) to give rise to drug-resistant recurrence [1,2]. The molecular mechanisms of cancer metastases are still under study but they are known to develop from small populations of cancer cells within a primary tumor, capable of entering and survive in the circulation and then exit to re-grow in a distant tissue [3]. The way the CSC theory may fit with the general scheme of metastatic potential is not well-defined to date.

Melanoma is a neoplasm stemming from melanocytes or the cells that develop from melanocytes, and since the increase in popularity of the CSC theory, single stem cells markers have been reported in the literature to correlate with melanoma malignancy, such as ABCB5, CD20, CD133, CD271, and ALDH1A [4]. These studies invite for further investigation about the potential role of stem cell pluripotency-related genes/proteins in its progression and potential metastatic transformation. Considering that stem cells (SCs) have the capability of self-renew and to differentiate into more specialized cells [5], the signaling pathways governing their properties are also subject of intense research. For instance, ion channels and its receptors, particularly, those responsible for calcium (Ca^{2+}) signal generation, are critical for determining cellular fate and differentiation of SCs and transcriptional changes in members of Ca^{2+} signaling pathway may thus trigger pathological events (*e.g.*, tumorigenesis) [6,7]. The possible link between intracellular Ca^{2+} and metastasis of human cancer cells is still poorly comprehended. A recent study (2016) by Rizaner and colleagues observed spontaneous Ca^{2+} oscillations in a proportion of strongly metastatic human prostate and breast cancer cells [8].

Probably, the biggest challenge for cancer researchers resides on the discovery of robust markers for prognosis and metastasis, in order to provide early diagnoses and treatment of patients.

The detection and follow-up of disease markers is nowadays based on solitary proteins, and this approach is most of the times unreliable. Wider and more powerful systems than conventional pathology-based data (e.g., immunohistochemical), capable of dealing and analyze increased amount of information are needed such as bioinformatics and systems biology tools [9]. For example, by the integration of additional information in biological pathways or a protein-protein interaction (PPI) network models, we could find "modular biomarkers" that integrate multiple genes with potential interactions that lead to more accurate and reproducible prognostic predictions and better comprehension of the disease pathogenesis [10]. In fact, our group has successfully applied network-based approaches and systems biology analyses in the context of diverse pathologies such as autism, Alzheimer's disease, and periodontal inflammation [11-17].

In this study, we created an integrated *in silico* network model of interactions in order to seek evidence for altered stem cell pluripotency and Ca^{+2} signaling pathways in microarray samples from three independent datasets of patients. By using a system biology-based approach, we search for de-regulated central genes at the transcriptional level that may represent putative biomarkers for melanoma metastases. Based on our findings, we hypothesize that aberrant signaling of stem cell pluripotency and Ca^{+2} pathways may account for metastatic transformation, and specifically propose 9 representative central genes of our whole interactomic model as optimal candidate group of biomarkers for human metastatic melanoma.

2. Material and methods

2.1 Development of the gene/protein interaction network model, data acquisition and processing

In order to build our integrated *in silico* network model ("STEMCa"), we first retrieved all genes annotated as members of the KEGG PATHWAY Database entries x and y, which are respectively "Signaling pathways regulating pluripotency of stem cells" (map04550) and " Ca^{2+} signaling pathway"

(map04020) (**Supplementary table 1**). The human interactome (*i.e.*, annotated interactions between human proteins) was downloaded from STRING V10.0 database (<http://string-db.org/>) [18] in a text file and read into the R programming environment, where scripts were written to generate our PPI network. We only used interactions reported by STRING as being from either “database” or “experimental evidence” and also with a minimum score of 0.400 (medium confidence). The basic steps for network generation were as follows: (i) proteins encoded by the KEGG gene list were used as input to build the PPI network with the set parameters; (ii) the algorithm searches for disconnected nodes on the network (*i.e.*, proteins with no reported interaction with the main network); (iii) if there are disconnected nodes, the algorithm will hunt for neighbor proteins that could be included into the network, or “connectors” (CONs) with the purpose of joining disconnected nodes to the main network; (iv) if two or more nodes are able to join a set of disconnected nodes to the main network, then the one with the highest degree is selected; and finally, (v) the algorithm only stops when there are no more nodes that can be added. The rationale behind this approach is to build a fully connected PPI network model from a list of protein with the least interference possible from *outsiders* (proteins that were not originally inputs) without losing network density connection.

2.2 Relative gene expression network visualization and microarray analysis

For our expression meta-analysis, we searched for cancer microarray raw data on GEO database (<http://www.ncbi.nlm.nih.gov/geo/>) by using as keywords: “melanoma” and “metastasis” or “metastatic melanoma” in *Homo sapiens*. Selected GSEs were GSE8401 (N=83), GSE46517 (N=104), GSE15605 (N=58). The database is publicly available and data were originally contributed by Xu et al. (2008) [19], Kabbarah et al. (2010) [20], and Raskin et al. (2013) [21], respectively. Experimental assays are explained in detail in these original publications; including the selection criteria of patients. Raw data was normalized by the use of robust array normalization (RMA). Differential gene expression analysis was performed through the implemented functions for R on the *limma* package,

which uses linear models to calculate moderated t-statistics for microarray data. The p -values were adjusted for multiple comparisons by calculating false discovery rates (FDR) [22]. Only genes reporting corrected p -values <0.05 (FDR) were considered to be differentially expressed (**Supplementary table 2**). Log fold changes for each of the encoding genes of the proteins on our *in silico* model were exported from R into text files and plotted over the PPI network (metastatic vs. primary melanoma samples) by using the plugin GALANT (GrAph LANdscape VisualizaTION) for Cytoscape (gaussian function sigma set to 0.04), which builds functional landscapes onto biological networks [23].

2.3 Elucidation of the topological network properties (degree or connectivity and betweenness)

Elucidation of the topological network properties [24] such as *degree* (also known as *connectivity*) and *betweenness* centralities (**Supplementary table 2**) was performed by using the Network Analyzer plugin from the Cytoscape software. Values of centralities above one standard deviation (+1SD) of the mean were selected to identify central nodes within the interactome. *Degree* gives information about the local topology of each node by summing up the number of its adjacent nodes. Nodes with high values of *degree* over the thresholds values are known as “hubs”. *Betweenness* provides values about how frequently the shortest path, connecting every pair of nodes, is going through a third given node. Therefore, *betweenness* provides information about the influence of a node over the spread of information throughout the interactome. Nodes with values of *betweenness* over the thresholds are named as “bottlenecks” (non-hub and hub-bottlenecks are represented by NH-Bs and HBs, respectively).

3. Results

3.1 “STEMCa” is an integrative network model of interactions for stem cell pluripotency and Ca^{+2} signaling pathways

Two pathways, the stem cell pluripotency (map04550) and Ca^{2+} signaling (map04020) (Supplementary table 1) are integrated within the interactome (Fig. 1), being composed of 294 nodes interconnecting through 2995 interactions. In the case of non-existing direct crosstalk through common members from both signaling pathways, it is possible to search for common neighboring nodes corresponding to additional genes/proteins or CONs to members of both pathways by the use of mathematical algorithms in the R environment (see “Material and methods” section). Our model included 21 CON within the “STEMCa” interactome.

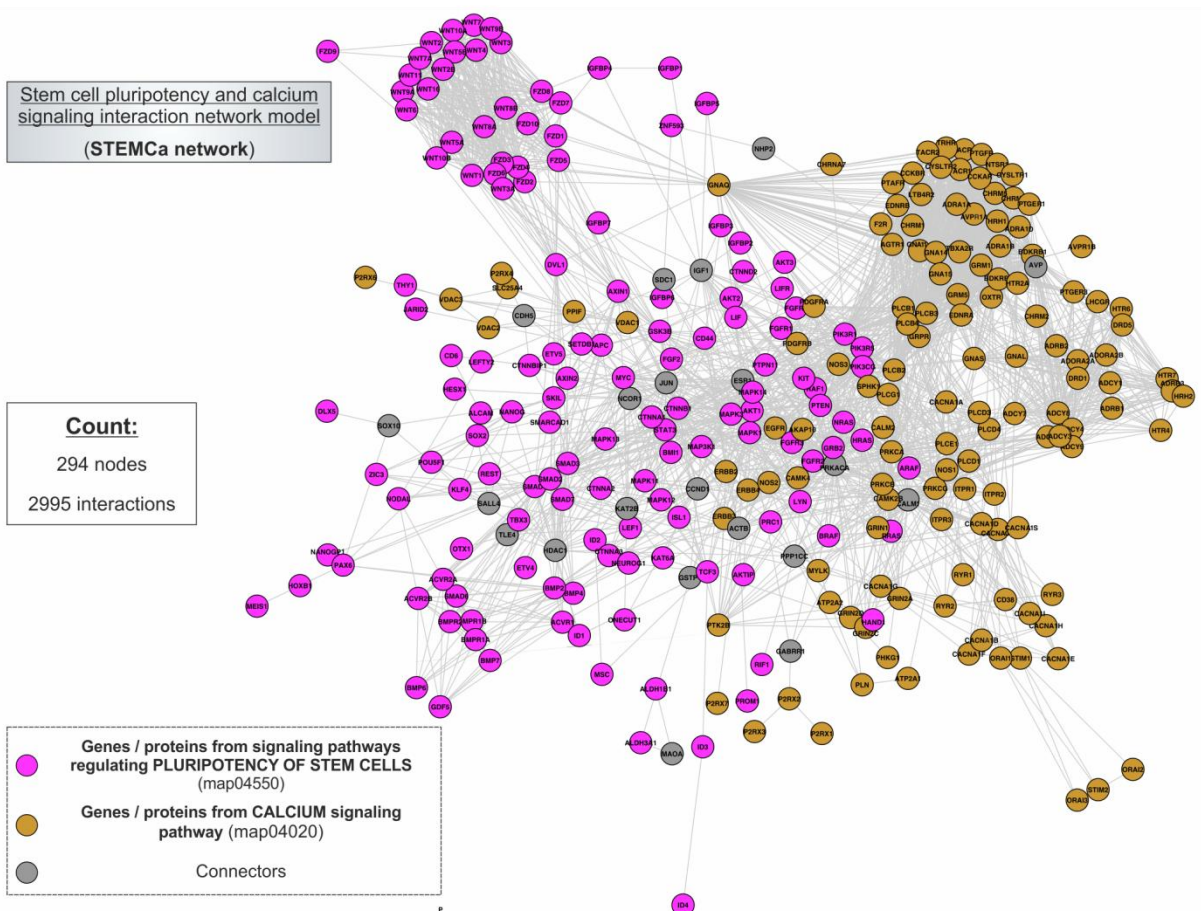


Figure 1. “STEMCa” interactome. General landscape of interactions between genes/proteins of stem cell pluripotency (map04550) and calcium signaling (map04020) interaction network model. The present *in silico* network model was developed by using the STRING V10.0 database resource search tool, exclusively using “Experiments” and “Databases” as input options for active prediction methods and a minimum confidence score of 0.400 (medium confidence).

3.2 Network-based analyses of stem cell pluripotency and Ca^{+2} signaling pathways reveal transcriptional changes in independent datasets of human metastatic melanoma

We performed a systems level analysis of potential transcriptional changes in genes belonging to SC pluripotency and Ca^{+2} signaling pathways in metastatic melanomas. The “STEMCa” interactome (Fig. 2A) was subjected to relative gene expression analysis profile by using the GALANT software, which plotted the expression mean values derived from metastatic melanoma over the expression of primary tumor samples in the network model, presenting it as two dimensional GALANT-generated landscapes graded by colors (Fig. 2B-D). The relative gene expression levels are color-coded with warm colors (yellow-red) being representative of higher expression, whereas cold (green-blue) colors represent lower gene expression, when compared to control samples.

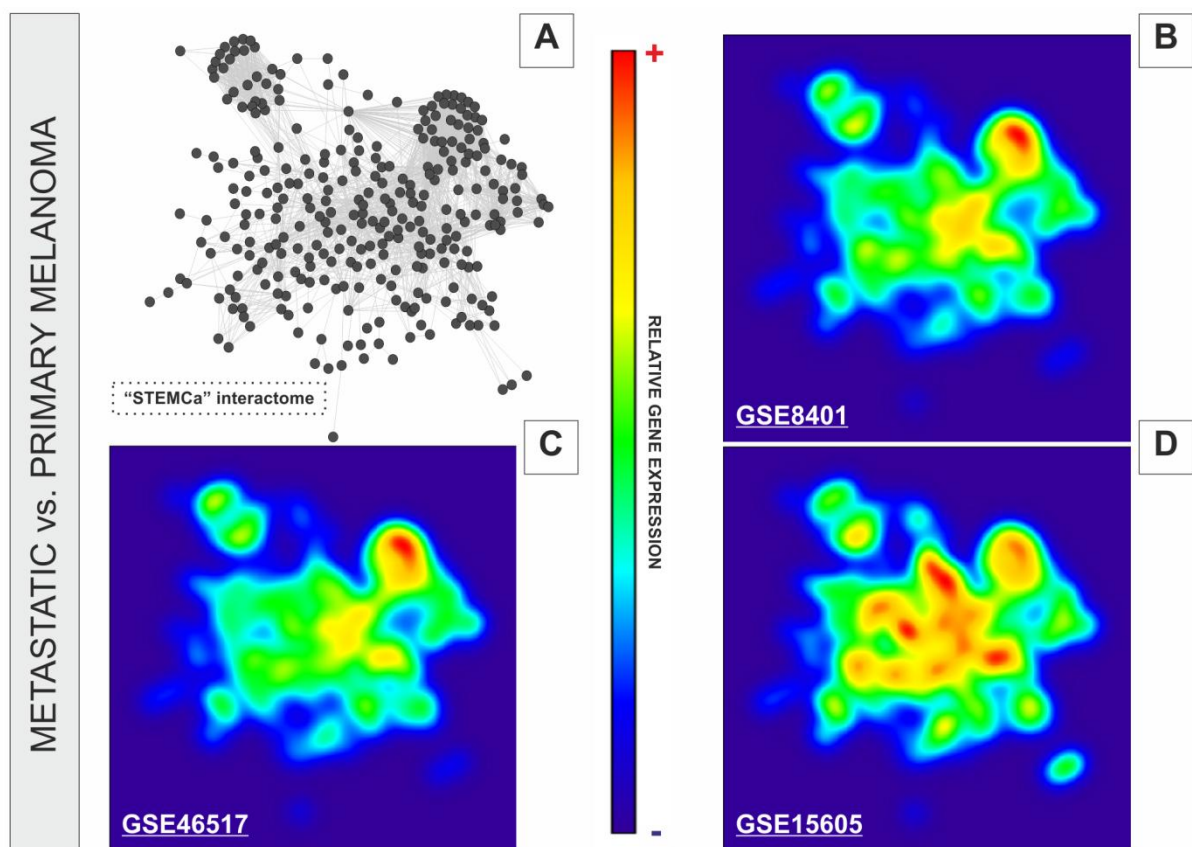


Figure 2. GALANT plots over the *in silico* model “STEMCa” in melanoma metastases from three independent sample sources from GEO. The figure represents the relative gene expression over the “STEMCa” interactome (A) in melanoma metastases vs. primary melanoma analyzed in (B) GSE8401, (C) GSE46517, and (D) GSE15605 independent micro-array samples, by using the GALANT software which is an open-source application able to build landscape maps of gene expression networks.

The 2D GALANT plots revealed equal landscape pattern of de-regulated relative gene expression in SC pluripotency and Ca²⁺ signaling pathways when metastatic melanomas were compared to primary tumors in three independent datasets (GSE8401, GSE46517, and GSE15605) of microarray samples (**Fig. 2B-D**). Differential expression analysis of “STEMCa” interactome revealed significant transcriptional changes in metastatic melanoma. In particular, 151 (~51%), 63 (~22%), and 14 (~5%) out of 294 genes from “STEMCa” interactome are differentially expressed (corrected *p*-values <0.05; FDR) in these tissue samples from one, two, or three independent microarray datasets, respectively (**Supplementary table 2**). At this stringent FDR, none of these changes were expected to be a false-positive. Of note, in all cases these genes follow the same pattern of de-regulation (up- or down-regulation) when datasets are compared (**Supplementary table 2** and **fig. 2**). The observed changes may account for the metastatic transformation of human melanoma with consequent alterations in patient survival.

3.3 Elucidation of key hub genes/proteins within the integrative “STEMCa” interactome suggest a group of candidate biomarkers for metastatic melanoma

For characterizing the newly-developed interactome, we calculated the topological network properties or centrality values (**Supplementary table 2**), in particular *degree* or *connectivity* and *betweenness*. These values reveal the most central nodes (genes/proteins) in a network [14-16]. Central nodes (NH-B and HB) mark points of “vulnerability” within the network of interactions and could consider that any variations in these members (*e.g.*, up- or down- regulation of given gene) can trigger more intense changes in the rest of the members of the interactome (*e.g.*, “STEMCa”) than those in non- or less central nodes. Therefore, one could consider that any gene/protein identified as NH-B or HB may represent one putative biomarker [16], especially if those showed the same qualitative up- or down-regulation in gene expression (corrected *p*-values <0.05; FDR), validated in at least two independent datasets of microarray samples. After calculating centrality values for the 294

“STEMCa” gene/protein members (**Supplementary table 2**), we identified 27 central nodes (**Fig. 3**), 19 NH-Bs (values of *betweenness* above one standard deviation of the mean) and 8 HBs (values of *betweenness* and *degree* above one standard deviation of the mean).

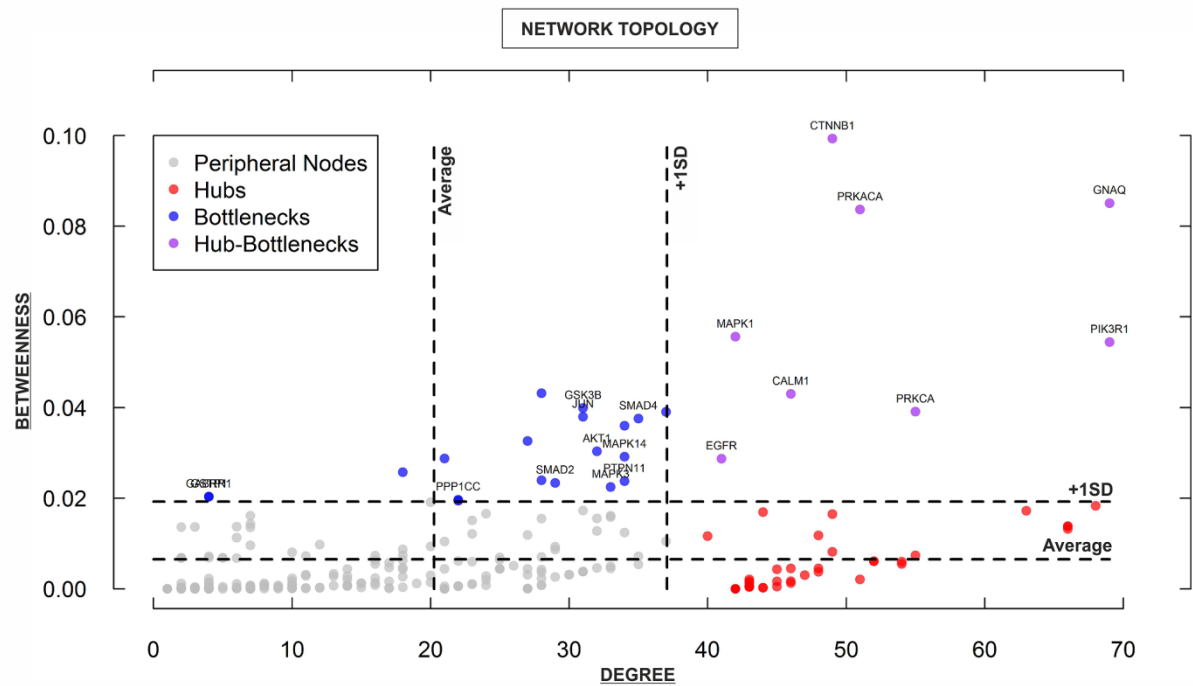


Figure 3. Analysis of the topological properties (*betweenness* vs. *degree*) of genes/proteins belonging to the “STEMCa” interactome. The figure identifies only central nodes, hub-bottlenecks (HBs) and non-hub-bottlenecks (NH-Bs) with values above +1SD of the mean, which are differentially expressed (corrected *p*-values <0.05) in at least one GSE from the re-analyzed cohorts (GSE8401, GSE46517, and GSE15605).

Respectively, 11, 5, and 1 gene/s out of 19 NH-Bs showed same qualitative (up- or down-regulation) differential gene expression (corrected *p*-values <0.05; FDR) in these tissue samples from one, two, or even three independent microarray datasets. 8 and 3 out of 8 HBs showed same qualitative differential gene expression (corrected *p*-values <0.05; FDR) in 1 or 2 GSEs datasets (**Table 1**). In particular, *CTNNB1*, *GNAQ*, *GSK3B*, *GSTP1*, *MAPK3*, *PPP1CC*, *PRKACA*, and *SMAD4* genes (corrected *p*-value <0.05; FDR) are over- or sub-expressed in at least 2 datasets of melanoma metastases when compared with primary tumor samples. Exclusively *PTPN11* or protein tyrosine phosphatase, non-receptor type 11 showed up-regulation (corrected *p*-value <0.05; FDR) in the three re-analyzed cohorts of patients (**Table 1**).

GENE INFORMATION			TOPOLOGY		NH -B HB	GSE8401		GSE46517		GSE15605	
Gene Symbol	Ensemble ID	Sub .	Degree	Betweenness		Diff. Exp.	Corrected <i>p</i> -value (FDR)	Diff. Exp.	Corrected <i>p</i> -value (FDR)	Diff . Exp .	Corrected <i>p</i> -value (FDR)
<i>AKT1</i>	ENSP00000270202	ST	32	0.0303424 7	NH -B	---	0.0730948 59	Down	0.00257 2769	---	0.9915918 7
<i>CALM1</i>	ENSP00000349467	CON	46	0.0429752 2	HB	---	0.4206402 18	Up	0.01435 4422	---	0.1027534 45
<i>CTNNB1</i>	ENSP00000344456	ST	49	0.0993434 6	HB	Up	0.0001128 83	Up	5.22113 E-05	---	0.1347369 08
<i>EGFR</i>	ENSP00000275493	Ca	41	0.0286749 6	HB	---	0.4544698 06	Down	4.09354 E-18	---	0.3729531 88
<i>ESR1</i>	ENSP00000206249	CON	37	0.0390276 2	NH -B	---	0.3436180 1	---	0.69191 3409	---	0.8583568 32
<i>GABRR1</i>	ENSP00000412673	CON	4	0.0203375 6	NH -B	---	0.5167505 81	---	0.17880 7962	Up	0.0302361 48
<i>GNAQ</i>	ENSP00000286548	Ca	69	0.0850879 7	HB	Up	0.0147697 85	Up	0.03812 2837	---	0.1747774 85
<i>GSK3B</i>	ENSP00000324806	ST	31	0.0398595 4	NH -B	Down	4.43231E- 06	Down	2.75596 E-10	---	0.5426678 81
<i>GSTP1</i>	ENSP00000381607	CON	4	0.0203375 6	NH -B	Down	3.14081E- 05	Down	2.61693 E-06	---	0.2744348 46
<i>HDAC1</i>	ENSP00000362649	CON	27	0.0326208 4	NH -B	---	0.2134344 49	---	0.71099 9269	---	0.8651720 09
<i>IGF1</i>	ENSP00000302665	CON	28	0.0431220 5	NH -B	---	0.6972660 13	---	0.43146 5367	---	0.6695677 5
<i>ITPR3</i>	ENSP00000363435	Ca	22	0.0194236 4	NH -B	---	0.2696230 07	---	0.67187 5922	---	0.7425626 21
<i>JUN</i>	ENSP00000360266	CON	31	0.0379296 2	NH -B	Down	8.92807E- 06	---	0.17136 6276	---	0.9006566 82
<i>MAPK1</i>	ENSP00000215832	ST	42	0.0556142 3	HB	Up	0.0004121 72	---	0.42909 1242	---	0.6084605 69
<i>MAPK14</i>	ENSP00000229794	ST	34	0.0291248 8	NH -B	---	0.6057388 21	Up	0.03864 2425	---	0.3587662 87
<i>MAPK3</i>	ENSP00000263025	ST	33	0.0224454 5	NH -B	Down	1.10052E- 05	Down	0.01074 679	---	0.9993195 65
<i>MYC</i>	ENSP00000367207	ST	34	0.0359844 1	NH -B	---	0.6028362 01	---	0.27405 7104	---	0.4496156 47
<i>NCOR1</i>	ENSP00000268712	CON	21	0.0287508 1	NH -B	---	0.6273518 08	---	0.25784 9878	---	0.1488311 32
<i>PIK3R1</i>	ENSP00000274335	ST	69	0.0544123 6	HB	---	0.3839065 59	Down	0.03005 9149	---	0.0578255 54
<i>PPP1CC</i>	ENSP00000335084	CON	22	0.0196550 9	NH -B	Up	1.52233E- 05	Up	3.22551 E-05	---	0.3079974 32
<i>PRKACA</i>	ENSP00000309591	CON	51	0.0837037	HB	Down	0.0019389 8	Down	0.00616 6758	---	0.0569472 92
<i>PRKCA</i>	ENSP00000408695	Ca	55	0.0390666 4	HB	Up	0.0038609 94	---	0.22782 6787	---	0.9342206 79
<i>PTPN11</i>	ENSP00000340944	ST	34	0.0237421 9	NH -B	Up	0.0399083 43	Up	0.00909 2992	Up	0.0482640 37
<i>SMAD2</i>	ENSP00000262160	ST	29	0.0233658 8	NH -B	Up	0.0094664 33	---	0.92471 9732	---	0.2329617 9
<i>SMAD3</i>	ENSP00000332973	ST	28	0.0239253 1	NH -B	---	0.9756475 88	---	0.09794 078	---	0.2198629 18
<i>SMAD4</i>	ENSP00000341551	ST	35	0.0375362 4	NH -B	Up	5.56315E- 06	Up	0.00029 2094	---	0.1414172 42
<i>TCF3</i>	ENSP00000262965	ST	18	0.0257338 4	NH -B	---	0.8034812 48	---	0.21713 9092	---	0.2601913 49
MEAN			20.3741 4	6.56E-03							
SD			16.8055 3	0.0127607 0							
MEAN +1SD			37.1796 8	0.0193220 3							

Table 1. Centrality values (*degree* and *betweenness*) for each node (gene/protein) within the stem cell pluripotency (map04550) and calcium signaling (map04020) interaction network model (“STEMCa” network). Differentially expressed genes within these members are listed. Centralities over the thresholds with value/s above one (+1SD) standard deviation of the mean are color-marked. Corrected *p*-values <0.05 were considered significant for differentially expressed genes. Nodes identified as non-hub-bottlenecks and hub-bottlenecks (based on *degree* and *betweenness* centralities), with values above +1SD of the mean, are represented as NH-B and HB, respectively. “ST”, “Ca”, and “CON” represent stem cell pluripotency, calcium signaling, and connector, respectively. NH-B and HB differentially expressed in at least two analyzed GSEs are underlined. Only one gene (*PTPN11*, NH-B) is differentially expressed (up-regulated) in the three analyzed GSEs. Table sorted by alphabetical order of gene symbol.

4. Discussion

In this piece, we have constructed an *in silico* interactome model resulting from the interplay between stem cell pluripotency and Ca^{2+} signaling pathways, in a network composed by 294 genes/proteins and 2995 interactions based on “Experiments” and “Databases” and a confidence score of at least 0.400 (**Fig. 1**). The newly-developed model was then subjected to further analysis by the GALANT software, showing a similar pattern of differences when relative expression of metastatic melanoma from three microarray datasets was plotted over the expression of primary tumor samples in the “STEMCa” interactome (**Fig. 2**). Differential expression analysis of “STEMCa” model showed significant transcriptional differences in metastatic vs. primary tumor tissues with around 51% (151 out of 294) exhibiting significant changes in at least one of the studied datasets (**Supplementary table 2**). In particular, *CTNNB1*, *GNAQ*, *GSK3B*, *GSTP1*, *MAPK3*, *PPP1CC*, *PRKACA*, *SMAD4*, and *PTPN11* are de-regulated (corrected *p*-values <0.05) central genes from our model in these tissue samples (**Table 1** and **Fig. 3**), representing not only a putative group of biomarkers but also potential therapeutic targets for melanoma metastases. The observed transcriptional changes may account for the molecular changes involved in metastatic transformation of primary tumor sites.

Melanoma is the most lethal type of skin cancer with around 73,870 estimated new cases in 2015; 9,940 people died due to this disease representing 4.5 % of all new cancer cases and its incidence is rising [25]. Metastasis is the spread of cancer cells from their primary tumor to distant organs and accounts for more than 90% of deaths in cancer patients since the majority of metastases are undetectable by clinicians [3,26]. Therefore, better comprehension of the mechanisms governing melanoma metastasis and the discovery of optimal biomarkers for early diagnoses remain necessary.

In general a couple of hallmarks make CSCs putative candidates to be responsible for cancer metastases: Firstly, it seems that only CSCs within tumors are capable of initiating and maintaining cancer growth and second, a single CSC is able develop a metastatic lesion, in contrast to the rest of cancer cells from the heterogenous tumor [27,28]. In addition, it has been reported the expression of

pluripotency markers in CSCs, which share a number of the molecular characteristics typical of normal SCs and also depend on typically embryonic signaling pathways. These molecular pathways likely represent novel therapeutic targets that could improve the rates of survival in patients [29].

The homeostasis of Ca^{2+} and Ca^{2+} -dependent signaling are critical components of cellular fate [30]. Surprisingly, this event have not been studied in detail yet as in pluripotent SCs. With all, it is known the role of Ca^{2+} signaling in both proliferation and differentiation of SCs at the very early stages of development and consequently, the fate of their physiopathological status *in vivo* [31]. Therefore, one could speculate whether transcriptional differences in stem cell pluripotency and Ca^{2+} signaling-related genes may contribute to the metastatic transformation in melanoma malignancy. The results we here present, derived from our newly-developed *in silico* model (**Fig. 1** and **supplementary table 1**), corroborate such hypothesis in three independent datasets of microarray samples (**Fig. 2** and **supplementary table 2**). However, the absence of experiments confirming the up- or down-regulation of these genes at the protein level in additional human metastatic melanoma tissues remains a limitation that requires further study.

Considering that diseases treated in the early stage are the ones with the greatest probability of success, the discovery of new melanoma biomarkers (genomics, proteomics, metabolomics) with the aid of OMICS and systems biology tools are required, in order to assist clinicians in the diagnose, follow-up, treatment, and even prediction of melanoma outcomes [32]. The use of PPI offers the opportunity to analyze the functional relationships among biological molecules within one or numerous signaling pathways [16], Once alterations at the transcriptional level are confirmed, in a given biological process/es, researchers can elucidate centrality values as a network-based approach to objectively identify/select candidate biomarkers and therapeutic targets *in silico* in the context of any disease [16,33,34]. In our study, we identified a group of central members such as *CTNNB1*, *GNAQ*, *GSK3B*, *GSTP1*, *MAPK3*, *PPP1CC*, *PRKACA*, *SMAD4*, and *PTPN11* genes within our *in silico* “STEMCa” interatomic model (**Fig. 3**). Thereafter, we qualitatively validated in at least two

independent datasets of patients from GEO significant differences in expression (corrected p -value <0.05 ; FDR) (**Table 1**). From those, only *PTPN11* (NH-B) gene confirmed its up-regulation in the three cohorts of patients. This could be due to the lower number of samples provided in the third re-analyzed dataset with 58 samples (GSE15605), when compared with the other two GSEs with 83 and 104 samples, respectively. This group of nine genes/proteins, as central (NH-Bs and HBs) down-regulated nodes occupying “vulnerable” points of “STEMCa” interactome, could represent potential therapeutic targets for melanoma metastases *in silico*, and invites for further investigation *in vitro* and *in vivo*.

PTPN11 gene encodes for the protein tyrosine phosphatase non-receptor type 11 and has subnetwork contribution to the “STEMCa” interactome from the stem cell pluripotency signaling pathway (map04550) (**Supplementary table 1**). It is remarkable that suppression of *PTPN11* confers sensitivity to BRAF inhibitors (used in cancer therapeutics) in colon cancer, by blocking signaling from receptor tyrosine kinases to the RAS-MEK-ERK pathway. This suppression also prevents the acquired resistance to targeted cancer drugs that results from receptor tyrosine kinase activation [35]. According to the CSC theory, one of the main characteristics of these cells is confer drug-resistant recurrence [1,2] and these recent findings [35] are therefore consistent with network-based identification of biomarkers and potential therapeutic targets from stem cell pluripotency and calcium signaling pathways in metastatic melanomas.

We conclude that (i) altered expression of stem cell pluripotency and Ca^{2+} signaling pathways-related genes may contribute to the metastatic transformation, and (ii) *CTNNB1*, *GNAQ*, *GSK3B*, *GSTP1*, *MAPK3*, *PPP1CC*, *PRKACA*, *SMAD4*, and especially *PTPN11* may represent an optimal candidate group of biomarkers and *in silico* therapeutic targets for melanoma metastasis.

5. References

- [1] E. Koren, Y. Fuchs, The bad seed: Cancer stem cells in tumor development and resistance, *Drug Resist Updat.* 28 (2012) 1-12.
- [2] J.D. Lathia, Cancer stem cells: moving past the controversy, *CNS Oncol.* 2 (2013) 465-467.
- [3] I.J. Fidler, The pathogenesis of cancer metastasis: the 'seed and soil' hypothesis revisited, *Nat Rev Cancer.* 3 (2003) 453-458.
- [4] Z. Kozovska, V. Gabrisova, L. Kucerova, Malignant melanoma: diagnosis, treatment and cancer stem cells, *Neoplasma.* 63 (2016) 510-517.
- [5] F. Zeidán-Chuliá, M. Noda, "Opening" the mesenchymal stem cell tool box, *Eur J Dent.* 3 (2009) 240-249.
- [6] G. Dayanithi, A. Verkhatsky, Calcium signalling in stem cells: Molecular physiology and multiple roles, *Cell Calcium.* 59 (2016) 55-56.
- [7] B. Kadio, S. Yaya, A. Basak, K. Djè, J. Gomes, C. Mesenge, Calcium role in human carcinogenesis: a comprehensive analysis and critical review of literature, *Cancer Metastasis Rev.* 35 (2016) 391-411.
- [8] N. Rizaner, R. Onkal, S.P. Fraser, A. Pristerá, K. Okuse, M.B. Djamgoz, Intracellular calcium oscillations in strongly metastatic human breast and prostate cancer cells: control by voltage-gated sodium channel activity, *Eur Biophys J.* 45 (2016) 735-748.
- [9] D.J. Johann Jr, M.D. McGuigan, A.R. Patel et al., Clinical proteomics and biomarker discovery, *Ann N Y Acad Sci.* 1022 (2004) 295-305.

- [10] N. Khunlertgit, B.J. Yoon, Incorporating topological information for predicting robust cancer subnetwork markers in human protein-protein interaction network, *BMC Bioinformatics*. 17 (2016) 351.
- [11] F. Zeidán-Chuliá, J.L Rybarczyk-Filho, M. Gursoy et al., Bioinformatical and in vitro approaches to essential oil-induced matrix metalloproteinase inhibition, *Pharm Biol*. 50 (2012) 675-686. doi: 10.3109/13880209.2012.677847.
- [12] F. Zeidán-Chuliá, B.H. Neves de Oliveira, M. Gursoy et al., MMP-REDOX/NO interplay in periodontitis and its inhibition with *Satureja hortensis* L. essential oil, *Chem Biodivers*. 10 (2013) 507-523. doi: 10.1002/cbdv.201200375.
- [13] F. Zeidán-Chuliá, M. Gursoy, B.H. de Oliveira et al., Focussed microarray analysis of apoptosis in periodontitis and its potential pharmacological targeting by carvacrol, *Arch Oral Biol*. 59 (2014) 461-469. doi: 10.1016/j.archoralbio.2014.01.007.
- [14] F. Zeidán-Chuliá, J.L. Rybarczyk-Filho, A.B. Salmina, B.H. de Oliveira, M. Noda, J.C. Moreira, Exploring the multifactorial nature of autism through computational systems biology: calcium and the Rho GTPase RAC1 under the spotlight, *Neuromolecular Med*. 15 (2013) 364-383. doi: 10.1007/s12017-013-8224-3.
- [15] F. Zeidán-Chuliá, B.H. de Oliveira, A.B Salmina et al., Altered expression of Alzheimer's disease-related genes in the cerebellum of autistic patients: a model for disrupted brain connectome and therapy, *Cell Death Dis*. 5 (2014) e1250. doi: 10.1038/cddis.2014.227.
- [16] F. Zeidán-Chuliá, M. Gürsoy, B.H. Neves de Oliveira, V. Özdemir, E. Könönen, U.K. Gürsoy, A Systems Biology Approach to Reveal Putative Host-Derived Biomarkers of Periodontitis by Network Topology Characterization of MMP-REDOX/NO and Apoptosis Integrated Pathways, *Front Cell Infect Microbiol*. 5 (2016) 102. doi: 10.3389/fcimb.2015.00102.

- [17] F. Zeidán-Chuliá F, B.H. de Oliveira, M.F. Casanova et al., Up-Regulation of Oligodendrocyte Lineage Markers in the Cerebellum of Autistic Patients: Evidence from Network Analysis of Gene Expression, *Mol Neurobiol.* 53 (2016) 4019-4025. doi: 10.1007/s12035-015-9351-7.
- [18] D. Szklarczyk, A. Franceschini, M. Kuhn et al., The STRING database in 2011: Functional interaction networks of proteins, globally integrated and scored, *Nucleic Acids Res.* 39 (2011) D561-D568.
- [19] L. Xu, S.S. Shen, Y. Hoshida et al., Gene expression changes in an animal melanoma model correlate with aggressiveness of human melanoma metastases, *Mol Cancer Res.* 6 (2008) 760-769.
- [20] O. Kabbarah, C. Nogueira, B. Feng et al., Integrative genome comparison of primary and metastatic melanomas, *PLoS One.* 5 (2010) e10770.
- [21] L. Raskin, D.R. Fullen, T.J. Giordano et al., Transcriptome profiling identifies HMGA2 as a biomarker of melanoma progression and prognosis, *J Invest Dermatol.* 133 (2013) 2585-2592.
- [22] Y. Pawitan, S. Michiels, S. Koscielny, A. Gusnanto, A. Ploner, False discovery rate, sensitivity and sample size for microarray studies, *Bioinformatics.* 21 (2005) 3017-3024.
- [23] E. Camilo, L.A. Bovolenta, M.L. Acencio, J.L. Rybarczyk-Filho, M.A. Castro, J.C. Moreira et al., GALANT: a Cytoscape plugin for visualizing data as functional landscapes projected onto biological networks, *Bioinformatics.* 29 (2013) 2505-2506.
- [24] H. Yu, P.M. Kim, E. Sprecher, V. Trifonov, M. Gerstein, The importance of bottlenecks in protein networks: correlation with gene essentiality and expression dynamics, *PLoS Comput Biol.* 3 (2007) e59.
- [25] L.S. Rebecca, D.M. Kimberly, J.Ahmedin, *Cancer Statistics, 2015, CA Cancer J Clin.* 65 (2015) 5-29.
- [26] A.F. Chambers, A.C. Groom, I.C. MacDonald, Dissemination and growth of cancer cells in metastatic sites, *Nat Rev Cancer.* 2 (2002) 563-572.

- [27] F. Li, B. Tiede, J. Massagué, Y. Kang, Beyond tumorigenesis: cancer stem cells in metastasis, *Cell Res.* 17 (2007) 3-14.
- [28] I.J. Fidler, J.E. Talmadge, Evidence that intravenously derived murine pulmonary melanoma metastases can originate from the expansion of a single tumor cell, *Cancer Res.* 46 (1986) 5167-5171.
- [29] O. Oren, B.D. Smith, Eliminating Cancer Stem Cells by Targeting Embryonic Signaling Pathways, *Stem Cell Rev.* (2016) doi: 10.1007/s12015-016-9691-3.
- [30] Á. Apáti, T. Berez, B. Sarkadi, Calcium signaling in human pluripotent stem cells, *Cell Calcium.* 59 (2016) 117-123.
- [31] O. Forostyak, S. Forostyak, S. Kortus, E. Sykova, A. Verkhatsky, G. Dayanithi, Physiology of Ca(2+) signalling in stem cells of different origins and differentiation stages, *Cell Calcium.* 59 (2016) 57-66.
- [32] S.B. Nimse, M.D. Sonawane, K.S. Song, T. Kim, Biomarker detection technologies and future directions, *Analyst.* 141 (2016) 740-755.
- [33] C.P. Cheng, I.Y. Kuo, H. Alakus et al., Network-based analysis identifies epigenetic biomarkers of esophageal squamous cell carcinoma progression, *Bioinformatics.* 30 (2014) 3054-3061.
- [34] J.O Rosado, J.P. Henriques, D. Bonatto. A systems pharmacology analysis of major chemotherapy combination regimens used in gastric cancer treatment: predicting potential new protein targets and drugs, *Curr Cancer Drug Targets.* 11 (2011) 849-869.
- [35] A. Prahallad, G.J. Heynen, G. Germano et al., PTPN11 Is a Central Node in Intrinsic and Acquired Resistance to Targeted Cancer Drugs, *Cell Rep.* 12 (2015) 1978-1985.

6. Supplementary Material

Supplementary table 1. Genes/proteins belonging to the stem cell pluripotency (map04550) and calcium signaling (map04020) interaction network model (“STEMCa” network) and its gene subnetwork contributions (stem cell pluripotency, “ST”; calcium signaling “Ca”; connector “CON”).

Gene Symbol	Ensemble ID	Description	Subnetwork Contribution
<i>ACTB</i>	ENSP00000349960	Actin, beta	CON
<i>ACVR1</i>	ENSP00000263640	Activin A receptor, type I	ST
<i>ACVR2A</i>	ENSP00000241416	Activin A receptor, type IIA	ST
<i>ACVR2B</i>	ENSP00000340361	Activin A receptor, type IIB	ST
<i>ADCY1</i>	ENSP00000297323	Adenylate cyclase 1 (brain)	Ca
<i>ADCY2</i>	ENSP00000342952	Adenylate cyclase 2 (brain)	Ca
<i>ADCY3</i>	ENSP00000260600	Adenylate cyclase 3	Ca
<i>ADCY4</i>	ENSP00000312126	Adenylate cyclase 4	Ca
<i>ADCY7</i>	ENSP00000254235	Adenylate cyclase 7	Ca
<i>ADCY8</i>	ENSP00000286355	Adenylate cyclase 8 (brain)	Ca
<i>ADCY9</i>	ENSP00000294016	Adenylate cyclase 9	Ca
<i>ADORA2A</i>	ENSP00000336630	Adenosine A2a receptor	Ca
<i>ADORA2B</i>	ENSP00000304501	Adenosine A2b receptor	Ca
<i>ADRA1A</i>	ENSP00000369960	Adrenoceptor alpha 1A	Ca
<i>ADRA1B</i>	ENSP00000306662	Adrenoceptor alpha 1B	Ca
<i>ADRA1D</i>	ENSP00000368766	Adrenoceptor alpha 1D	Ca
<i>ADRB1</i>	ENSP00000358301	Adrenoceptor beta 1	Ca
<i>ADRB2</i>	ENSP00000305372	Adrenoceptor beta 2	Ca
<i>ADRB3</i>	ENSP00000343782	Adrenoceptor beta 3	Ca
<i>AGTR1</i>	ENSP00000273430	Angiotensin II receptor, type 1	Ca
<i>AKAP10</i>	ENSP00000225737	A kinase (PRKA) anchor protein 10	Ca
<i>AKT1</i>	ENSP00000270202	v-akt murine thymoma viral oncogene homolog 1	ST
<i>AKT2</i>	ENSP00000375892	v-akt murine thymoma viral oncogene homolog 2	ST
<i>AKT3</i>	ENSP00000263826	v-akt murine thymoma viral oncogene homolog 3 (protein kinase B, gamma)	ST
<i>AKTIP</i>	ENSP00000378152	AKT interacting protein	ST
<i>ALCAM</i>	ENSP00000305988	Activated leukocyte cell adhesion molecule	ST
<i>ALDH1B1</i>	ENSP00000366927	Aldehyde dehydrogenase 1 family, member B1	ST
<i>ALDH3A1</i>	ENSP00000225740	Aldehyde dehydrogenase 3 family, member A1	ST
<i>APC</i>	ENSP00000257430	Adenomatous polyposis coli	ST
<i>ARAF</i>	ENSP00000366244	v-raf murine sarcoma 3611 viral	ST

		oncogene homolog	
<i>ATP2A1</i>	ENSP00000349595	ATPase, Ca ⁺⁺ transporting, cardiac muscle, fast twitch 1	Ca
<i>ATP2A2</i>	ENSP00000440045	ATPase, Ca ⁺⁺ transporting, cardiac muscle, slow twitch 2	Ca
<i>AVP</i>	ENSP00000369647	Arginine vasopressin	CON
<i>AVPR1A</i>	ENSP00000299178	Arginine vasopressin receptor 1A	Ca
<i>AVPR1B</i>	ENSP00000356094	Arginine vasopressin receptor 1B	Ca
<i>AXIN1</i>	ENSP00000262320	Axin 1	ST
<i>AXIN2</i>	ENSP00000302625	Axin 2	ST
<i>BDKRB1</i>	ENSP00000216629	Bradykinin receptor B1	Ca
<i>BDKRB2</i>	ENSP00000307713	Bradykinin receptor B2	Ca
<i>BMI1</i>	ENSP00000365851	BMI1 polycomb ring finger oncogene	ST
<i>BMP2</i>	ENSP00000368104	Bone morphogenetic protein 2	ST
<i>BMP4</i>	ENSP00000245451	Bone morphogenetic protein 4	ST
<i>BMP6</i>	ENSP00000283147	Bone morphogenetic protein 6	ST
<i>BMP7</i>	ENSP00000379204	Bone morphogenetic protein 7	ST
<i>BMPRI1A</i>	ENSP00000224764	Bone morphogenetic protein receptor, type IA	ST
<i>BMPRI1B</i>	ENSP00000264568	Bone morphogenetic protein receptor, type IB	ST
<i>BMPRI2</i>	ENSP00000363708	Bone morphogenetic protein receptor, type II (serine/threonine kinase)	ST
<i>BRAF</i>	ENSP00000288602	v-raf murine sarcoma viral oncogene homolog B1	ST
<i>CACNA1A</i>	ENSP00000353362	Calcium channel, voltage-dependent, P/Q type, alpha 1A subunit	Ca
<i>CACNA1B</i>	ENSP00000360406	Calcium channel, voltage-dependent, N type, alpha 1B subunit	Ca
<i>CACNA1C</i>	ENSP00000266376	Calcium channel, voltage-dependent, L type, alpha 1C subunit	Ca
<i>CACNA1D</i>	ENSP00000288139	Calcium channel, voltage-dependent, L type, alpha 1D subunit	Ca
<i>CACNA1E</i>	ENSP00000356545	Calcium channel, voltage-dependent, R type, alpha 1E subunit	Ca
<i>CACNA1F</i>	ENSP00000365441	Calcium channel, voltage-dependent, L type, alpha 1F subunit	Ca
<i>CACNA1G</i>	ENSP00000352011	Calcium channel, voltage-dependent, T type, alpha 1G subunit	Ca
<i>CACNA1H</i>	ENSP00000334198	Calcium channel, voltage-dependent, T type, alpha 1H subunit	Ca
<i>CACNA1I</i>	ENSP00000385019	Calcium channel, voltage-dependent, T type, alpha 1I subunit	Ca
<i>CACNA1S</i>	ENSP00000355192	Calcium channel, voltage-dependent, L type, alpha 1S subunit	Ca
<i>CALM1</i>	ENSP00000349467	Calmodulin 1 (phosphorylase kinase, delta)	CON
<i>CALM2</i>	ENSP00000272298	Calmodulin 2 (phosphorylase kinase, delta)	Ca

<i>CAMK2B</i>	ENSP00000379098	Calcium/calmodulin-dependent protein kinase II beta	Ca
<i>CAMK4</i>	ENSP00000282356	Calcium/calmodulin-dependent protein kinase IV	Ca
<i>CCKAR</i>	ENSP00000295589	Cholecystokinin A receptor	Ca
<i>CCKBR</i>	ENSP00000335544	Cholecystokinin B receptor	Ca
<i>CCND1</i>	ENSP00000227507	Cyclin D1	CON
<i>CD38</i>	ENSP00000226279	CD38 molecule	Ca
<i>CD44</i>	ENSP00000398632	CD44 molecule (Indian blood group)	ST
<i>CD6</i>	ENSP00000323280	CD6 molecule	ST
<i>CDH5</i>	ENSP00000344115	Cadherin 5, type 2 (vascular endothelium)	CON
<i>CHRM1</i>	ENSP00000306490	Cholinergic receptor, muscarinic 1	Ca
<i>CHRM2</i>	ENSP00000319984	Cholinergic receptor, muscarinic 2	Ca
<i>CHRM3</i>	ENSP00000255380	Cholinergic receptor, muscarinic 3	Ca
<i>CHRM5</i>	ENSP00000372750	Cholinergic receptor, muscarinic 5	Ca
<i>CHRNA7</i>	ENSP00000407546	Cholinergic receptor, nicotinic, alpha 7 (neuronal)	Ca
<i>CTNNA1</i>	ENSP00000304669	Catenin (cadherin-associated protein), alpha 1, 102kDa	ST
<i>CTNNA2</i>	ENSP00000418191	Catenin (cadherin-associated protein), alpha 2	ST
<i>CTNNA3</i>	ENSP00000362849	Catenin (cadherin-associated protein), alpha 3	ST
<i>CTNNB1</i>	ENSP00000344456	Catenin (cadherin-associated protein), beta 1, 88kDa	ST
<i>CTNNBIP1</i>	ENSP00000366466	Catenin, beta interacting protein 1	ST
<i>CTNND2</i>	ENSP00000307134	Catenin (cadherin-associated protein), delta 2	ST
<i>CYSLTR1</i>	ENSP00000362401	Cysteinyl leukotriene receptor 1	Ca
<i>CYSLTR2</i>	ENSP00000282018	Cysteinyl leukotriene receptor 2	Ca
<i>DLX5</i>	ENSP00000222598	Distal-less homeobox 5	ST
<i>DRD1</i>	ENSP00000327652	Dopamine receptor D1	Ca
<i>DRD5</i>	ENSP00000306129	Dopamine receptor D5	Ca
<i>DVL1</i>	ENSP00000368169	Dishevelled, dsh homolog 1 (Drosophila)	ST
<i>EDNRA</i>	ENSP00000315011	Endothelin receptor type A	Ca
<i>EDNRB</i>	ENSP00000366416	Endothelin receptor type B	Ca
<i>EGFR</i>	ENSP00000275493	Epidermal growth factor receptor	Ca
<i>ERBB2</i>	ENSP00000269571	v-erb-b2 erythroblastic leukemia viral oncogene homolog 2, neuro/glioblastoma derived oncogene homolog (avian)	Ca
<i>ERBB3</i>	ENSP00000267101	v-erb-b2 erythroblastic leukemia viral oncogene homolog 3 (avian)	Ca
<i>ERBB4</i>	ENSP00000342235	v-erb-a erythroblastic leukemia viral oncogene homolog 4 (avian)	Ca
<i>ESR1</i>	ENSP00000206249	Estrogen receptor 1	CON
<i>ETV4</i>	ENSP00000321835	Ets variant 4	ST

<i>ETV5</i>	ENSP00000306894	Ets variant 5	ST
<i>F2R</i>	ENSP00000321326	Coagulation factor II (thrombin) receptor	Ca
<i>FGF2</i>	ENSP00000264498	Fibroblast growth factor 2 (basic)	ST
<i>FGFR1</i>	ENSP00000393312	Fibroblast growth factor receptor 1	ST
<i>FGFR2</i>	ENSP00000410294	Fibroblast growth factor receptor 2	ST
<i>FGFR3</i>	ENSP00000339824	Fibroblast growth factor receptor 3	ST
<i>FGFR4</i>	ENSP00000292408	Fibroblast growth factor receptor 4	ST
<i>FZD1</i>	ENSP00000287934	Frizzled family receptor 1	ST
<i>FZD10</i>	ENSP00000229030	Frizzled family receptor 10	ST
<i>FZD2</i>	ENSP00000323901	Frizzled family receptor 2	ST
<i>FZD3</i>	ENSP00000240093	Frizzled family receptor 3	ST
<i>FZD4</i>	ENSP00000434034	Frizzled family receptor 4	ST
<i>FZD5</i>	ENSP00000354607	Frizzled family receptor 5	ST
<i>FZD6</i>	ENSP00000351605	Frizzled family receptor 6	ST
<i>FZD7</i>	ENSP00000286201	Frizzled family receptor 7	ST
<i>FZD8</i>	ENSP00000363826	Frizzled family receptor 8	ST
<i>FZD9</i>	ENSP00000345785	Frizzled family receptor 9	ST
<i>GABRR1</i>	ENSP00000412673	Gamma-aminobutyric acid (GABA) A receptor, rho 1	CON
<i>GDF5</i>	ENSP00000363489	Growth differentiation factor 5	ST
<i>GNA11</i>	ENSP00000078429	Guanine nucleotide binding protein (G protein), alpha 11 (Gq class)	Ca
<i>GNA14</i>	ENSP00000365807	Guanine nucleotide binding protein (G protein), alpha 14	Ca
<i>GNA15</i>	ENSP00000262958	Guanine nucleotide binding protein (G protein), alpha 15 (Gq class)	Ca
<i>GNAL</i>	ENSP00000334051	Guanine nucleotide binding protein (G protein), alpha activating activity polypeptide, olfactory type	Ca
<i>GNAQ</i>	ENSP00000286548	Guanine nucleotide binding protein (G protein), q polypeptide	Ca
<i>GNAS</i>	ENSP00000360141	GNAS complex locus	Ca
<i>GRB2</i>	ENSP00000339007	Growth factor receptor-bound protein 2	ST
<i>GRIN1</i>	ENSP00000360608	Glutamate receptor, ionotropic, N-methyl D-aspartate 1	Ca
<i>GRIN2A</i>	ENSP00000332549	Glutamate receptor, ionotropic, N-methyl D-aspartate 2A	Ca
<i>GRIN2C</i>	ENSP00000293190	Glutamate receptor, ionotropic, N-methyl D-aspartate 2C	Ca
<i>GRIN2D</i>	ENSP00000263269	Glutamate receptor, ionotropic, N-methyl D-aspartate 2D	Ca
<i>GRM1</i>	ENSP00000282753	Glutamate receptor, metabotropic 1	Ca
<i>GRM5</i>	ENSP00000306138	Glutamate receptor, metabotropic 5	Ca
<i>GRPR</i>	ENSP00000369643	Gastrin-releasing peptide receptor	Ca
<i>GSK3B</i>	ENSP00000324806	Glycogen synthase kinase 3 beta	ST
<i>GSTP1</i>	ENSP00000381607	Glutathione S-transferase pi 1	CON
<i>HAND1</i>	ENSP00000231121	Heart and neural crest derivatives expressed 1	ST

<i>HDAC1</i>	ENSP00000362649	Histone deacetylase 1	CON
<i>HESX1</i>	ENSP00000295934	HESX homeobox 1	ST
<i>HOXB1</i>	ENSP00000355140	Homeobox B1	ST
<i>HRAS</i>	ENSP00000309845	v-Ha-ras Harvey rat sarcoma viral oncogene homolog	ST
<i>HRH1</i>	ENSP00000380247	Histamine receptor H1	Ca
<i>HRH2</i>	ENSP00000366506	Histamine receptor H2	Ca
<i>HTR2A</i>	ENSP00000367959	5-hydroxytryptamine (serotonin) receptor 2A, G protein-coupled	Ca
<i>HTR4</i>	ENSP00000353915	5-hydroxytryptamine (serotonin) receptor 4, G protein-coupled	Ca
<i>HTR6</i>	ENSP00000289753	5-hydroxytryptamine (serotonin) receptor 6, G protein-coupled	Ca
<i>HTR7</i>	ENSP00000337949	5-hydroxytryptamine (serotonin) receptor 7, adenylate cyclase-coupled	Ca
<i>ID1</i>	ENSP00000365280	Inhibitor of DNA binding 1, dominant negative helix-loop-helix protein	ST
<i>ID2</i>	ENSP00000234091	Inhibitor of DNA binding 2, dominant negative helix-loop-helix protein	ST
<i>ID3</i>	ENSP00000363689	Inhibitor of DNA binding 3, dominant negative helix-loop-helix protein	ST
<i>ID4</i>	ENSP00000367972	Inhibitor of DNA binding 4, dominant negative helix-loop-helix protein	ST
<i>IGF1</i>	ENSP00000302665	Insulin-like growth factor 1 (somatomedin C)	CON
<i>IGFBP1</i>	ENSP00000275525	Insulin-like growth factor binding protein 1	ST
<i>IGFBP2</i>	ENSP00000233809	Insulin-like growth factor binding protein 2, 36kDa	ST
<i>IGFBP3</i>	ENSP00000370473	Insulin-like growth factor binding protein 3	ST
<i>IGFBP4</i>	ENSP00000269593	Insulin-like growth factor binding protein 4	ST
<i>IGFBP5</i>	ENSP00000233813	Insulin-like growth factor binding protein 5	ST
<i>IGFBP6</i>	ENSP00000301464	Insulin-like growth factor binding protein 6	ST
<i>IGFBP7</i>	ENSP00000295666	Insulin-like growth factor binding protein 7	ST
<i>ISL1</i>	ENSP00000230658	ISL LIM homeobox 1	ST
<i>ITPR1</i>	ENSP00000306253	Inositol 1,4,5-trisphosphate receptor, type 1	Ca
<i>ITPR2</i>	ENSP00000370744	Inositol 1,4,5-trisphosphate receptor, type 2	Ca
<i>ITPR3</i>	ENSP00000363435	Inositol 1,4,5-trisphosphate receptor, type 3	Ca
<i>JARID2</i>	ENSP00000341280	Jumonji, AT rich interactive domain 2	ST
<i>JUN</i>	ENSP00000360266	Jun proto-oncogene	CON
<i>KAT2B</i>	ENSP00000263754	K(lysine) acetyltransferase 2B	CON

<i>KAT6A</i>	ENSP00000265713	K(lysine) acetyltransferase 6A	ST
<i>KIT</i>	ENSP00000288135	v-kit Hardy-Zuckerman 4 feline sarcoma viral oncogene homolog	ST
<i>KLF4</i>	ENSP00000363804	Kruppel-like factor 4 (gut)	ST
<i>LEF1</i>	ENSP00000265165	Lymphoid enhancer-binding factor 1	ST
<i>LEFTY2</i>	ENSP00000355785	Left-right determination factor 2	ST
<i>LHCGR</i>	ENSP00000294954	Luteinizing hormone/choriogonadotropin receptor	Ca
<i>LIF</i>	ENSP00000249075	Leukemia inhibitory factor	ST
<i>LIFR</i>	ENSP00000263409	Leukemia inhibitory factor receptor alpha	ST
<i>LTB4R2</i>	ENSP00000433290	Leukotriene B4 receptor 2	Ca
<i>LYN</i>	ENSP00000428924	v-yes-1 Yamaguchi sarcoma viral related oncogene homolog	ST
<i>MAOA</i>	ENSP00000340684	Monoamine oxidase A	CON
<i>MAP3K1</i>	ENSP00000382423	Mitogen-activated protein kinase kinase kinase 1, E3 ubiquitin protein ligase	ST
<i>MAPK1</i>	ENSP00000215832	Mitogen-activated protein kinase 1	ST
<i>MAPK11</i>	ENSP00000333685	Mitogen-activated protein kinase 11	ST
<i>MAPK12</i>	ENSP00000215659	Mitogen-activated protein kinase 12	ST
<i>MAPK13</i>	ENSP00000211287	Mitogen-activated protein kinase 13	ST
<i>MAPK14</i>	ENSP00000229794	Mitogen-activated protein kinase 14	ST
<i>MAPK3</i>	ENSP00000263025	Mitogen-activated protein kinase 3	ST
<i>MEIS1</i>	ENSP00000272369	Meis homeobox 1	ST
<i>MSC</i>	ENSP00000321445	Musculin	ST
<i>MYC</i>	ENSP00000367207	v-myc myelocytomatosis viral oncogene homolog (avian)	ST
<i>MYLK</i>	ENSP00000353452	Myosin light chain kinase	Ca
<i>NANOG</i>	ENSP00000229307	Nanog homeobox	ST
<i>NANOGP1</i>	ENSP00000432545	Nanog homeobox pseudogene 1	ST
<i>NCOR1</i>	ENSP00000268712	Nuclear receptor corepressor 1	CON
<i>NEUROG1</i>	ENSP00000317580	Neurogenin 1	ST
<i>NHP2</i>	ENSP00000274606	NHP2 ribonucleoprotein homolog (yeast)	CON
<i>NODAL</i>	ENSP00000287139	Nodal homolog (mouse)	ST
<i>NOS1</i>	ENSP00000337459	Nitric oxide synthase 1 (neuronal)	Ca
<i>NOS2</i>	ENSP00000327251	Nitric oxide synthase 2, inducible	Ca
<i>NOS3</i>	ENSP00000297494	Nitric oxide synthase 3 (endothelial cell)	Ca
<i>NRAS</i>	ENSP00000358548	Neuroblastoma RAS viral (v-ras) oncogene homolog	ST
<i>NTSR1</i>	ENSP00000359532	Neurotensin receptor 1 (high affinity)	Ca
<i>ONECUT1</i>	ENSP00000302630	One cut homeobox 1	ST
<i>ORAI1</i>	ENSP00000328216	ORAI calcium release-activated calcium modulator 1	Ca
<i>ORAI2</i>	ENSP00000348752	ORAI calcium release-activated calcium modulator 2	Ca
<i>ORAI3</i>	ENSP00000322249	ORAI calcium release-activated calcium modulator 3	Ca
<i>OTX1</i>	ENSP00000282549	Orthodenticle homeobox 1	ST

<i>OXTR</i>	ENSP00000324270	Oxytocin receptor	Ca
<i>P2RX1</i>	ENSP00000225538	Purinergic receptor P2X, ligand-gated ion channel, 1	Ca
<i>P2RX2</i>	ENSP00000343339	Purinergic receptor P2X, ligand-gated ion channel, 2	Ca
<i>P2RX3</i>	ENSP00000263314	Purinergic receptor P2X, ligand-gated ion channel, 3	Ca
<i>P2RX4</i>	ENSP00000336607	Purinergic receptor P2X, ligand-gated ion channel, 4	Ca
<i>P2RX6</i>	ENSP00000416193	Purinergic receptor P2X, ligand-gated ion channel, 6	Ca
<i>P2RX7</i>	ENSP00000442349	Purinergic receptor P2X, ligand-gated ion channel, 7	Ca
<i>PAX6</i>	ENSP00000368401	Paired box 6	ST
<i>PDGFRA</i>	ENSP00000257290	Platelet-derived growth factor receptor, alpha polypeptide	Ca
<i>PDGFRB</i>	ENSP00000261799	Platelet-derived growth factor receptor, beta polypeptide	Ca
<i>PHKG1</i>	ENSP00000297373	Phosphorylase kinase, gamma 1 (muscle)	Ca
<i>PIK3CG</i>	ENSP00000352121	Phosphatidylinositol-4,5-bisphosphate 3-kinase, catalytic subunit gamma	ST
<i>PIK3R1</i>	ENSP00000274335	Phosphoinositide-3-kinase, regulatory subunit 1 (alpha)	ST
<i>PIK3R5</i>	ENSP00000392812	Phosphoinositide-3-kinase, regulatory subunit 5	ST
<i>PLCB1</i>	ENSP00000338185	Phospholipase C, beta 1 (phosphoinositide-specific)	Ca
<i>PLCB2</i>	ENSP00000260402	Phospholipase C, beta 2	Ca
<i>PLCB3</i>	ENSP00000279230	Phospholipase C, beta 3 (phosphatidylinositol-specific)	Ca
<i>PLCB4</i>	ENSP00000334105	Phospholipase C, beta 4	Ca
<i>PLCD1</i>	ENSP00000430344	Phospholipase C, delta 1	Ca
<i>PLCD3</i>	ENSP00000313731	Phospholipase C, delta 3	Ca
<i>PLCD4</i>	ENSP00000388631	Phospholipase C, delta 4	Ca
<i>PLCE1</i>	ENSP00000260766	Phospholipase C, epsilon 1	Ca
<i>PLCG1</i>	ENSP00000244007	Phospholipase C, gamma 1	Ca
<i>PLN</i>	ENSP00000350132	Phospholamban	Ca
<i>POU5F1</i>	ENSP00000259915	POU class 5 homeobox 1	ST
<i>PPIF</i>	ENSP00000225174	Peptidylprolyl isomerase F	Ca
<i>PPP1CC</i>	ENSP00000335084	Protein phosphatase 1, catalytic subunit, gamma isozyme	CON
<i>PRC1</i>	ENSP00000377793	Protein regulator of cytokinesis 1	ST
<i>PRKACA</i>	ENSP00000309591	Protein kinase, cAMP-dependent, catalytic, alpha	CON
<i>PRKCA</i>	ENSP00000408695	Protein kinase C, alpha	Ca
<i>PRKCB</i>	ENSP00000305355	Protein kinase C, beta	Ca
<i>PRKCG</i>	ENSP00000263431	Protein kinase C, gamma	Ca
<i>PROM1</i>	ENSP00000415481	Prominin 1	ST

<i>PTAFR</i>	ENSP00000301974	Platelet-activating factor receptor	Ca
<i>PTEN</i>	ENSP00000361021	Phosphatase and tensin homolog	ST
<i>PTGER1</i>	ENSP00000292513	Prostaglandin E receptor 1 (subtype EP1), 42kDa	Ca
<i>PTGER3</i>	ENSP00000349003	Prostaglandin E receptor 3 (subtype EP3)	Ca
<i>PTGFR</i>	ENSP00000359793	Prostaglandin F receptor (FP)	Ca
<i>PTK2B</i>	ENSP00000332816	PTK2B protein tyrosine kinase 2 beta	Ca
<i>PTPN11</i>	ENSP00000340944	Protein tyrosine phosphatase, non-receptor type 11	ST
<i>RAF1</i>	ENSP00000251849	v-raf-1 murine leukemia viral oncogene homolog 1	ST
<i>REST</i>	ENSP00000311816	RE1-silencing transcription factor	ST
<i>RIF1</i>	ENSP00000243326	RAP1 interacting factor homolog (yeast)	ST
<i>RRAS</i>	ENSP00000246792	Related RAS viral (r-ras) oncogene homolog	ST
<i>RYR1</i>	ENSP00000352608	Ryanodine receptor 1 (skeletal)	Ca
<i>RYR2</i>	ENSP00000355533	Ryanodine receptor 2 (cardiac)	Ca
<i>RYR3</i>	ENSP00000373884	Ryanodine receptor 3	Ca
<i>SALL4</i>	ENSP00000217086	Sal-like 4 (Drosophila)	CON
<i>SDC1</i>	ENSP00000254351	Syndecan 1	CON
<i>SETDB1</i>	ENSP00000271640	SET domain, bifurcated 1	ST
<i>SKIL</i>	ENSP00000259119	SKI-like oncogene	ST
<i>SLC25A4</i>	ENSP00000281456	Solute carrier family 25 (mitochondrial carrier; adenine nucleotide translocator), member 4	Ca
<i>SMAD2</i>	ENSP00000262160	SMAD family member 2	ST
<i>SMAD3</i>	ENSP00000332973	SMAD family member 3	ST
<i>SMAD4</i>	ENSP00000341551	SMAD family member 4	ST
<i>SMAD6</i>	ENSP00000288840	SMAD family member 6	ST
<i>SMAD7</i>	ENSP00000262158	SMAD family member 7	ST
<i>SMARCA1</i>	ENSP00000351947	SWI/SNF-related, matrix-associated actin-dependent regulator of chromatin, subfamily a, containing DEAD/H box 1	ST
<i>SOX10</i>	ENSP00000354130	SRY (sex determining region Y)-box 10	CON
<i>SOX2</i>	ENSP00000323588	SRY (sex determining region Y)-box 2	ST
<i>SPHK1</i>	ENSP00000313681	Sphingosine kinase 1	Ca
<i>STAT3</i>	ENSP00000264657	Signal transducer and activator of transcription 3 (acute-phase response factor)	ST
<i>STIM1</i>	ENSP00000300737	Stromal interaction molecule 1	Ca
<i>STIM2</i>	ENSP00000417569	Stromal interaction molecule 2	Ca
<i>TACR1</i>	ENSP00000303522	Tachykinin receptor 1	Ca
<i>TACR2</i>	ENSP00000362403	Tachykinin receptor 2	Ca
<i>TACR3</i>	ENSP00000303325	Tachykinin receptor 3	Ca
<i>TBX3</i>	ENSP00000257566	T-box 3	ST
<i>TBXA2R</i>	ENSP00000393333	Thromboxane A2 receptor	Ca
<i>TCF3</i>	ENSP00000262965	Transcription factor 3 (E2A immunoglobulin enhancer binding	ST

		factors E12/E47)	
<i>THY1</i>	ENSP00000284240	Thy-1 cell surface antigen	ST
<i>TLE4</i>	ENSP00000365735	Transducin-like enhancer of split 4 (E(sp1) homolog, Drosophila)	CON
<i>TRHR</i>	ENSP00000309818	Thyrotropin-releasing hormone receptor	Ca
<i>VDAC1</i>	ENSP00000265333	Voltage-dependent anion channel 1	Ca
<i>VDAC2</i>	ENSP00000361635	Voltage-dependent anion channel 2	Ca
<i>VDAC3</i>	ENSP00000428845	Voltage-dependent anion channel 3	Ca
<i>WNT1</i>	ENSP00000293549	Wingless-type MMTV integration site family, member 1	ST
<i>WNT10A</i>	ENSP00000258411	Wingless-type MMTV integration site family, member 10A	ST
<i>WNT10B</i>	ENSP00000301061	Wingless-type MMTV integration site family, member 10B	ST
<i>WNT11</i>	ENSP00000325526	Wingless-type MMTV integration site family, member 11	ST
<i>WNT16</i>	ENSP00000222462	Wingless-type MMTV integration site family, member 16	ST
<i>WNT2</i>	ENSP00000265441	Wingless-type MMTV integration site family member 2	ST
<i>WNT2B</i>	ENSP00000358698	Wingless-type MMTV integration site family, member 2B	ST
<i>WNT3</i>	ENSP00000225512	Wingless-type MMTV integration site family, member 3	ST
<i>WNT3A</i>	ENSP00000284523	Wingless-type MMTV integration site family, member 3A	ST
<i>WNT4</i>	ENSP00000290167	Wingless-type MMTV integration site family, member 4	ST
<i>WNT5A</i>	ENSP00000264634	Wingless-type MMTV integration site family, member 5A	ST
<i>WNT5B</i>	ENSP00000308887	Wingless-type MMTV integration site family, member 5B	ST
<i>WNT6</i>	ENSP00000233948	Wingless-type MMTV integration site family, member 6	ST
<i>WNT7A</i>	ENSP00000285018	Wingless-type MMTV integration site family, member 7A	ST
<i>WNT7B</i>	ENSP00000341032	Wingless-type MMTV integration site family, member 7B	ST
<i>WNT8A</i>	ENSP00000381739	Wingless-type MMTV integration site family, member 8A	ST
<i>WNT8B</i>	ENSP00000340677	Wingless-type MMTV integration site family, member 8B	ST
<i>WNT9A</i>	ENSP00000272164	Wingless-type MMTV integration site family, member 9A	ST
<i>WNT9B</i>	ENSP00000290015	Wingless-type MMTV integration site family, member 9B	ST
<i>ZIC3</i>	ENSP00000287538	Zic family member 3	ST
<i>ZNF593</i>	ENSP00000363384	Zinc finger protein 593	ST

Supplementary table 2. Centrality values (*degree* and *betweenness*) and differentially expressed genes from the stem cell pluripotency (map04550) and calcium signaling (map04020) interaction network model (“STEMCa” network). Corrected *p*-values <0.05 were considered significant. “ST”, “Ca”, and “CON” represent stem cell pluripotency, calcium signaling, and connector, respectively. Centralities over the thresholds with value/s above one (+1SD) standard deviation of the mean are color-marked.

GENE INFORMATION			TOPOLOGY		GSE8401			GSE46517			GSE15605		
Gene Symbol	Ensemble ID	Subnetwork	Degree	Betweenness	LogFC	Differential Exp.	Corrected p-value (FDR)	LogFC	Differential Exp.	Corrected p-value (FDR)	LogFC	Differential Exp.	Corrected p-value (FDR)
ACTB	ENSP00000349960	CON	20	0.01907129	-0.024108298	no	0.761449925	-0.00686	no	0.803684421	1.559675026	Up	0.032652195
ACVR1	ENSP00000263640	ST	11	0.00718543	0.493435774	Up	0.002341069	0.014872	no	0.750579897	0.259755304	no	0.395003714
ACVR2A	ENSP00000241416	ST	15	0.00119467	-0.0283413	no	0.677864084	0.017547	no	0.634267226	-0.456205804	no	0.088499856
ACVR2B	ENSP00000340361	ST	15	0.00119467	0.125032579	no	0.105642614	0.024948	no	0.4679031	0.475372468	no	0.181619371
ADCY1	ENSP00000297323	Ca	28	0.00226065	0.770309904	Up	0.003237809	0.129314	Up	0.04036285	0.250179176	no	0.8225865
ADCY2	ENSP00000342952	Ca	31	0.00377255	-0.816673844	Down	0.000913162	-0.3964	Down	4.27246E-06	-2.246747858	Down	0.019316464
ADCY3	ENSP00000260600	Ca	32	0.00459359	0.063873407	no	0.637425296	-0.04102	no	0.23974253	-0.130007519	no	0.769024733
ADCY4	ENSP00000312126	Ca	31	0.00377255	<i>no probe</i>	<i>no probe</i>	<i>no probe</i>	<i>no probe</i>	<i>no probe</i>	<i>no probe</i>	-0.963961392	Down	0.047564684
ADCY7	ENSP00000254235	Ca	32	0.01277469	-0.047589167	no	0.816569602	-0.07034	no	0.408955104	-0.210228945	no	0.601933035
ADCY8	ENSP00000286355	Ca	33	0.00446963	-0.174215996	Down	0.016616289	-0.06279	no	0.051168453	-0.335921631	no	0.247837447
ADCY9	ENSP00000294016	Ca	31	0.00377255	0.428191131	Down	0.01814938	0.18131	Down	0.015078196	0.519722729	no	0.103479907
ADORA2A	ENSP00000336630	Ca	23	0.00102844	<i>no probe</i>	<i>no probe</i>	<i>no probe</i>	<i>no probe</i>	<i>no probe</i>	<i>no probe</i>	<i>no probe</i>	<i>no probe</i>	<i>no probe</i>
ADORA2B	ENSP00000304501	Ca	22	0.000576	0.091943694	no	0.677859748	-0.03734	no	0.526103972	0.552891787	no	0.443724055
ADRA1A	ENSP00000369960	Ca	43	0.000634	-0.052828498	no	0.319141538	-0.07484	no	0.21525575	-0.206687591	no	0.347422003
ADRA1B	ENSP00000306662	Ca	46	0.00127274	0.056029792	no	0.299706925	0.029342	no	0.65009466	-0.111464079	no	0.586795269
ADRA1D	ENSP00000368766	Ca	43	0.000634	-0.073784386	no	0.379436234	-0.0444	no	0.377800315	-0.204841053	no	0.424114462
ADRB1	ENSP00000358301	Ca	24	0.00197701	-0.110653483	no	0.054753207	0.024246	no	0.6296024	0.675856475	no	0.416422134
ADRB	ENSP00000	Ca	29	0.00258	-	no	0.06054	-	no	0.18549	-	Down	0.0131

2	305372			616	0.23687 8921		8662	0.041 27		4082	1.52973 6243	wn	42131
ADRB 3	ENSP00000 343782	Ca	21	0.00000 275	- 0.02450 0254	no	0.74364 1898	0.100 18	no	0.05300 0578	- 0.38532 8567	no	0.1007 19202
AGTR 1	ENSP00000 273430	Ca	48	0.00448 218	- 0.05267 8124	no	0.73132 5344	0.088 783	no	0.22338 8799	0.24448 0193	no	0.7743 08308
AKAP 10	ENSP00000 225737	Ca	1	0	0.11176 6375	no	0.14278 6753	0.084 407	no	0.05202 8474	0.87140 7694	no	0.1485 02956
AKT1	ENSP00000 270202	ST	32	0.03034 247	- 0.24592 9347	no	0.07309 4859	- 0.118 25	Do wn	0.00257 2769	- 0.00455 5422	no	0.9915 9187
AKT2	ENSP00000 375892	ST	10	0.00172 914	0.00368 7556	no	0.97038 7807	- 0.054 44	no	0.41407 7105	0.47289 4843	no	0.2143 53755
AKT3	ENSP00000 263826	ST	6	0.00009 74	0.53815 105	Up	0.00024 0754	0.019 771	no	0.80083 1597	1.94695 9962	Up	0.0042 71082
AKTIP	ENSP00000 378152	ST	1	0	0.19260 4401	Do wn	0.01898 5222	- 0.060 75	no	0.07928 4466	0.14151 5237	no	0.6875 92363
ALCA M	ENSP00000 305988	ST	1	0	0.01430 6297	no	0.96087 0922	0.072 82	no	0.52421 4628	- 0.03479 6199	no	0.9618 46632
ALDH 1B1	ENSP00000 366927	ST	1	0	0.27180 7519	Up	0.01847 9944	0.084 034	no	0.10839 2189	0.17344 8261	no	0.7463 13451
ALDH 3A1	ENSP00000 225740	ST	2	0.01360 512	- 1.28140 477	Do wn	7.65086 E-14	0.369 27	Do wn	1.00595 E-14	- 1.66618 2948	Do wn	0.0124 65938
APC	ENSP00000 257430	ST	13	0.00330 135	0.04445 2604	no	0.39078 6804	0.071 77	no	0.17291 3743	0.84023 5375	no	0.1442 16088
ARAF	ENSP00000 366244	ST	10	0.00009 34	0.10216 7477	no	0.13460 5848	- 0.020 64	no	0.57008 4586	0.50696 9343	no	0.1907 50032
ATP2A 1	ENSP00000 349595	Ca	2	0.00005 75	- 0.03143 3038	no	0.74094 2807	0.023 71	no	0.74313 0158	- 0.25413 4846	no	0.2180 62139
ATP2A 2	ENSP00000 440045	Ca	3	0.00022 2	0.22505 9947	no	0.07450 3034	0.003 918	no	0.94478 3973	0.22349 7694	no	0.4151 18732
AVP	ENSP00000 369647	CON	63	0.01721 403	0.16039 8739	Do wn	0.00835 7143	0.039 159	no	0.36406 6614	0.08256 2994	no	0.6130 46328
AVPR 1A	ENSP00000 299178	Ca	43	0.00037 3	0.02537 9757	no	0.72690 2328	- 0.072 53	no	0.21341 6041	- 0.16885 8597	no	0.7427 0437
AVPR 1B	ENSP00000 356094	Ca	1	0	0.19423 6639	Do wn	0.00206 9273	0.017 751	no	0.63398 8754	- 0.15209 6423	no	0.4414 88605
AXIN1	ENSP00000 262320	ST	21	0.01043 37	0.10224 1516	no	0.08114 5394	0.039 99	no	0.13260 8851	- 0.34316 5433	no	0.2251 50251
AXIN2	ENSP00000 302625	ST	9	0.00023 8	<i>no probe</i>	<i>no pr ob e</i>	<i>no probe</i>	<i>no prob e</i>	<i>no pro be</i>	<i>no probe</i>	- 1.33914 3633	Do wn	0.0154 7958
BDKR B1	ENSP00000 216629	Ca	51	0.00208 106	- 0.14115 1364	Do wn	0.01723 9378	- 0.053 64	no	0.49368 9279	- 0.36495 9628	no	0.3227 24166
BDKR B2	ENSP00000 307713	Ca	54	0.00547 469	- 0.67796 8642	Do wn	1.24357 E-15	0.420 07	Do wn	1.38507 E-17	- 1.05612 7029	Do wn	0.0451 21581
BMI1	ENSP00000 365851	ST	4	0.00003 58	<i>no probe</i>	<i>no pr ob e</i>	<i>no probe</i>	<i>no prob e</i>	<i>no pro be</i>	<i>no probe</i>	<i>no probe</i>	<i>no pro be</i>	<i>no probe</i>
BMP2	ENSP00000 368104	ST	20	0.00935 5	0.22259 0883	no	0.29776 4194	0.043 115	no	0.59259 277	- 1.28833 4655	Do wn	0.0158 89038
BMP4	ENSP00000 245451	ST	16	0.00731 462	- 0.31036 2702	Do wn	0.00309 9308	- 0.471 96	Do wn	4.18036 E-05	- 0.81379 411	no	0.0949 84367
BMP6	ENSP00000 283147	ST	7	0.00000 425	0.12308 4462	no	0.28764 1243	0.093 497	no	0.16719 5897	0.52850 6397	no	0.2642 63554
BMP7	ENSP00000	ST	11	0.00017	-	no	0.24368	-	no	0.46218	0.07807	no	0.9557

	379204			4	0.08379 9725		6624	0.039 42		0145	5942		06107
<i>BMPR 1A</i>	ENSP00000 224764	ST	14	0.00073 5	0.14505 9004	no	0.05950 6879	- 0.018 56	no	0.82734 0048	0.57434 3394	no	0.1205 78819
<i>BMPR 1B</i>	ENSP00000 264568	ST	13	0.00065 9	0.13079 8092	no	0.13628 7556	0.069 788	no	0.12181 4471	- 1.47424 6454	no	0.0537 77794
<i>BMPR 2</i>	ENSP00000 363708	ST	14	0.00073 5	- 0.44833 6832	Do wn	0.00011 8576	- 0.231 17	Do wn	3.66751 E-07	0.86134 2009	no	0.0874 37272
<i>BRAF</i>	ENSP00000 288602	ST	14	0.00059 5	0.18663 9374	Up	0.00209 567	0.097 903	Up	0.00442 8605	0.65380 3191	no	0.2137 0785
<i>CACN A1A</i>	ENSP00000 353362	Ca	5	0.00040 3	- 0.03159 1228	no	0.75183 8231	- 0.175 86	Do wn	0.00477 2247	- 0.06493 1331	no	0.9057 52777
<i>CACN A1B</i>	ENSP00000 360406	Ca	7	0	- 0.24689 251	Do wn	0.00115 0002	0.033 64	no	0.46603 5081	- 0.56454 9564	no	0.1014 26239
<i>CACN A1C</i>	ENSP00000 266376	Ca	17	0.00571 8	- 0.09940 0691	no	0.17422 8705	- 0.098 54	no	0.06023 0691	- 0.41947 977	no	0.3747 48958
<i>CACN A1D</i>	ENSP00000 288139	Ca	16	0.00632 295	- 0.09540 7579	no	0.16938 6086	- 0.018 8	no	0.79817 9115	- 1.19305 511	no	0.0866 83789
<i>CACN A1E</i>	ENSP00000 356545	Ca	7	0	- 0.06264 8998	no	0.33242 6359	0.009 584	no	0.86223 7025	- 0.37641 9091	no	0.3248 10026
<i>CACN A1F</i>	ENSP00000 365441	Ca	7	0	0.11049 4279	no	0.18126 5161	- 0.055 71	no	0.31305 8214	- 0.21549 8325	no	0.2279 71683
<i>CACN A1G</i>	ENSP00000 352011	Ca	12	0.00971 323	- 0.07966 2181	no	0.19673 9841	- 0.032 26	no	0.68208 4341	- 0.55473 0986	no	0.1098 83555
<i>CACN A1H</i>	ENSP00000 334198	Ca	10	0.00090 1	- 0.14764 6031	Do wn	0.01810 3666	- 0.043 37	no	0.30367 4783	- 0.34407 4896	no	0.1465 01819
<i>CACN A1I</i>	ENSP00000 385019	Ca	7	0.00001 7	- 0.03094 2	no	0.68026 309	0.015 795	no	0.71555 4113	- 0.09490 9931	no	0.7833 93576
<i>CACN A1S</i>	ENSP00000 355192	Ca	14	0.00431 991	- 0.07798 1502	no	0.15958 4796	0.049 286	no	0.27855 8668	- 0.03348 1743	no	0.8453 26922
<i>CALM 1</i>	ENSP00000 349467	CON	46	0.04297 522	0.05970 491	no	0.42064 0218	0.082 097	Up	0.01435 4422	0.89879 6891	no	0.1027 53445
<i>CALM 2</i>	ENSP00000 272298	Ca	11	0.00310 394	<i>no probe</i>	<i>no probe</i>	<i>no probe</i>	<i>no probe</i>	<i>no probe</i>	<i>no probe</i>	<i>no probe</i>	<i>no probe</i>	<i>no probe</i>
<i>CAMK 2B</i>	ENSP00000 379098	Ca	29	0.00928 585	- 0.01718 0559	no	0.69625 2539	- 0.020 8	no	0.82545 0834	- 0.03600 4175	no	0.9342 38294
<i>CAMK 4</i>	ENSP00000 282356	Ca	7	0.00046 8	0.08255 3391	no	0.23578 7616	0.150 469	Up	0.00095 5151	0.21287 6403	no	0.8001 97653
<i>CCKA R</i>	ENSP00000 295589	Ca	42	0.00000 382	- 0.11422 2594	no	0.10669 6824	0.013 983	no	0.76901 408	- 0.04693 4205	no	0.9002 41907
<i>CCKB R</i>	ENSP00000 335544	Ca	43	0.00127 413	- 0.15080 949	Do wn	0.02570 3471	- 0.029 04	no	0.36897 5123	- 0.42354 9775	no	0.1655 28817
<i>CCND 1</i>	ENSP00000 227507	CON	18	0.00739 75	- 0.78659 9389	Do wn	0.00159 198	- 0.229 17	Do wn	0.00506 7749	- 0.10012 6092	no	0.8527 03841
<i>CD38</i>	ENSP00000 226279	Ca	6	0.00034 2	0.63316 3266	Up	0.00152 246	0.141 65	Up	0.00797 8865	1.37567 8242	Up	0.0053 07694
<i>CD44</i>	ENSP00000 398632	ST	10	0.00229 193	- 0.44306 1465	Do wn	0.02298 6638	0.131 686	no	0.17910 9005	0.49028 8672	no	0.4791 48798
<i>CD6</i>	ENSP00000 323280	ST	2	0.00682 594	- 0.40718 1124	Do wn	0.00299 8311	0.067 237	no	0.71128 1452	- 0.41558 4687	no	0.4960 54969
<i>CDH5</i>	ENSP00000 344115	CON	6	0.01369 088	- 0.22950 1486	no	0.13975 5758	- 0.271 5	Do wn	0.00019 8259	- 0.30548 2103	no	0.3901 22841

<i>CHRM 1</i>	ENSP00000306490	Ca	49	0.00816648	no probe	no probe	no probe	no probe	no probe	no probe	-0.848163445	no	0.08631478
<i>CHRM 2</i>	ENSP00000319984	Ca	16	0.000846	0.102543657	no	0.368022426	0.148074	Up	2.72041E-05	-0.141731168	no	0.446372646
<i>CHRM 3</i>	ENSP00000255380	Ca	44	0.000224	0.302635974	Up	0.033554266	0.048657	no	0.704420478	0.257621355	no	0.776247495
<i>CHRM 5</i>	ENSP00000372750	Ca	44	0.000224	0.086640245	no	0.35743343	0.064373	no	0.098808445	-0.211711882	no	0.325431383
<i>CHRN A7</i>	ENSP00000407546	Ca	1	0	no probe	no probe	no probe	no probe	no probe	no probe	no probe	no probe	no probe
<i>CTNN A1</i>	ENSP00000304669	ST	16	0.00547324	-0.423084932	Do wn	0.001525878	-0.09298	no	0.141453598	1.150609889	no	0.060574303
<i>CTNN A2</i>	ENSP00000418191	ST	8	0.000443	-0.146311509	no	0.189635269	0.044375	no	0.452861071	-0.081112324	no	0.920987621
<i>CTNN A3</i>	ENSP00000362849	ST	3	0.0000359	-0.034442392	no	0.606649134	-0.04157	no	0.268857768	-0.177100562	no	0.422572677
<i>CTNN B1</i>	ENSP00000344456	ST	49	0.09934346	0.573777007	Up	0.000112883	0.161343	Up	5.22113E-05	0.801985615	no	0.134736908
<i>CTNN BIP1</i>	ENSP00000366466	ST	7	0.000349	-0.771669249	Do wn	1.86249E-13	-0.27636	Do wn	5.36471E-16	-0.798545079	Do wn	0.031494238
<i>CTNN D2</i>	ENSP00000307134	ST	2	0.000215	-0.175894329	Do wn	0.000467185	0.03196	no	0.594139458	-0.568506595	no	0.275886549
<i>CYSLT R1</i>	ENSP00000362401	Ca	42	0.00000382	-0.066353691	no	0.059370283	0.042701	no	0.525517399	-0.359284529	no	0.425823745
<i>CYSLT R2</i>	ENSP00000282018	Ca	42	0.00000382	0.006319143	no	0.961072995	-0.01204	no	0.873988316	-0.645886751	no	0.233398296
<i>DLX5</i>	ENSP00000222598	ST	1	0	-0.268598333	Do wn	3.33381E-05	-0.01215	no	0.728025125	0.110247434	no	0.840731238
<i>DRD1</i>	ENSP00000327652	Ca	23	0.001007	0.013983884	no	0.787069697	0.102939	Up	0.016480638	-0.19250745	no	0.242391909
<i>DRD5</i>	ENSP00000306129	Ca	22	0.000576	0.055393592	no	0.592811441	0.005495	no	0.868778465	-0.01086879	no	0.946459053
<i>DVLI</i>	ENSP00000368169	ST	24	0.01655107	-0.251755594	Do wn	0.02991641	-0.04217	no	0.423828376	0.879342464	Do wn	0.004058239
<i>EDNR A</i>	ENSP00000315011	Ca	54	0.00594781	0.152646475	Do wn	0.00389713	-0.23916	Do wn	0.000373873	-0.463940959	no	0.454813356
<i>EDNR B</i>	ENSP00000366416	Ca	45	0.00161893	0.06962535	no	0.867511022	-0.03943	no	0.802086629	-0.165741295	no	0.788352776
<i>EGFR</i>	ENSP00000275493	Ca	41	0.02867496	-0.074739452	no	0.454469806	-0.77396	Do wn	4.09354E-18	-0.91200768	no	0.372953188
<i>ERBB 2</i>	ENSP00000269571	Ca	23	0.00599284	-0.771670613	Do wn	4.23948E-10	-0.29477	Do wn	1.84539E-10	-0.579780806	no	0.171349238
<i>ERBB 3</i>	ENSP00000267101	Ca	14	0.00208024	0.016327019	no	0.968562333	-0.04873	no	0.682084341	-0.016214834	no	0.984742649
<i>ERBB 4</i>	ENSP00000342235	Ca	18	0.00462692	0.145840034	no	0.060516277	-0.06295	no	0.122525084	0.129515459	no	0.898711344
<i>ESR1</i>	ENSP00000206249	CON	37	0.03902762	0.065573168	no	0.34361801	-0.03276	no	0.691913409	-0.121373719	no	0.858356832
<i>ETV4</i>	ENSP00000	ST	1	0	0.04648	no	0.79195	0.029	no	0.79411	1.03681	Up	0.0291

	321835				2663		8206	367		606	2913		15616
<i>ETV5</i>	ENSP00000 306894	ST	1	0	0.26018 9791	no	0.33458 146	- 0.149 35	no	0.06868 2414	1.20157 5161	no	0.0811 40066
<i>F2R</i>	ENSP00000 321326	Ca	48	0.01178 359	0.60224 3494	Up	0.02314 7566	0.108 833	no	0.17617 7758	- 0.53459 5111	no	0.3461 16148
<i>FGF2</i>	ENSP00000 264498	ST	14	0.00281 367	0.10692 3208	no	0.10148 6883	- 0.006	no	0.94613 3832	0.23002 0218	no	0.6927 80856
<i>FGFR 1</i>	ENSP00000 393312	ST	16	0.00132 134	- 0.16901 2033	no	0.38503 6119	- 0.171 79	no	0.05954 5658	0.02194 8761	no	0.9737 62337
<i>FGFR 2</i>	ENSP00000 410294	ST	16	0.00237 305	- 0.04378 8263	no	0.54666 231	- 0.491 96	Do wn	2.8766 E-13	- 2.89374 1608	Do wn	0.0062 70883
<i>FGFR 3</i>	ENSP00000 339824	ST	10	0.00046 5	- 2.51545 166	Do wn	4.2596 E-13	- 1.111 92	Do wn	7.5847 E-19	- 3.21433 5236	Do wn	0.0061 24764
<i>FGFR 4</i>	ENSP00000 292408	ST	9	0.00047 7	0.08437 7835	no	0.23026 2848	0.147 837	Up	0.02648 4362	- 0.27396 1519	no	0.3901 85329
<i>FZD1</i>	ENSP00000 287934	ST	25	0.00690 974	0.26987 118	no	0.25589 5831	0.040 916	no	0.69495 0224	0.64865 8056	no	0.0820 422
<i>FZD10</i>	ENSP00000 229030	ST	21	0.00437 685	- 0.71598 3427	Do wn	2.49109 E-11	- 0.326 64	Do wn	3.50974 E-15	- 1.52662 9405	Do wn	0.0232 53115
<i>FZD2</i>	ENSP00000 323901	ST	28	0.00702 029	0.08809 5883	no	0.41064 1519	0.005 88	no	0.92062 2314	0.55937 1415	no	0.0810 95083
<i>FZD3</i>	ENSP00000 240093	ST	25	0.00437 685	0.24364 8857	Up	0.00769 8645	0.132 634	Up	0.00038 6567	0.60034 5554	no	0.1846 91037
<i>FZD4</i>	ENSP00000 434034	ST	27	0.00438 291	- 0.03535 3176	no	0.70435 913	- 0.047 27	no	0.07546 9187	- 0.40331 0645	no	0.2458 60687
<i>FZD5</i>	ENSP00000 354607	ST	31	0.01723 32	- 0.07236 8926	no	0.29149 4394	0.064 076	no	0.14874 996	0.39486 6852	no	0.3555 91884
<i>FZD6</i>	ENSP00000 351605	ST	25	0.00437 685	0.47645 0171	no	0.07513 5475	- 0.018 69	no	0.83981 9858	- 0.50021 6734	no	0.2541 36444
<i>FZD7</i>	ENSP00000 286201	ST	25	0.00437 986	0.42773 233	no	0.08084 5101	0.051 32	no	0.64761 7036	- 0.18018 4209	no	0.7501 11855
<i>FZD8</i>	ENSP00000 363826	ST	25	0.00637 76	- 0.04034 2841	no	0.67344 977	0.001 689	no	0.97769 6363	0.18464 1108	no	0.8146 32786
<i>FZD9</i>	ENSP00000 345785	ST	3	0	- 0.06503 9336	no	0.58237 7552	0.056 973	no	0.36392 4495	0.01902 3728	no	0.9667 47866
<i>GABR R1</i>	ENSP00000 412673	CON	4	0.02033 756	0.04355 3532	no	0.51675 0581	0.045 095	no	0.17880 7962	0.97027 7925	Up	0.0302 36148
<i>GDF5</i>	ENSP00000 363489	ST	9	0.00001 48	0.00803 7279	no	0.92324 5213	0.017 108	no	0.80068 4561	- 0.10036 6752	no	0.5903 68797
<i>GNA1 1</i>	ENSP00000 078429	Ca	52	0.00607 334	- 0.13974 6345	no	0.24700 3933	0.412 342	Up	0.00011 1027	0.04113 9788	no	0.9296 93492
<i>GNA1 4</i>	ENSP00000 365807	Ca	52	0.00607 334	0.08739 7394	no	0.23504 3887	- 0.054 62	no	0.32115 1731	0.17571 6186	no	0.7468 73279
<i>GNA1 5</i>	ENSP00000 262958	Ca	55	0.00734 64	- 1.28355 2441	Do wn	1.41761 E-13	- 0.569 68	Do wn	1.24793 E-15	- 1.22725 2208	Do wn	0.0425 81416
<i>GNAL</i>	ENSP00000 334051	Ca	28	0.00363 512	0.61190 0981	Do wn	0.00342 7336	- 0.694 32	Do wn	6.07879 E-09	- 1.08082 8356	no	0.1311 20178
<i>GNAQ</i>	ENSP00000 286548	Ca	69	0.08508 797	0.29848 7114	Up	0.01476 9785	0.073 427	Up	0.03812 2837	0.74299 322	no	0.1747 77485
<i>GNAS</i>	ENSP00000 360141	Ca	40	0.01161 783	0.11680 9053	no	0.29739 8232	- 0.088 81	no	0.15406 3105	0.49692 8684	no	0.3511 57727
<i>GRB2</i>	ENSP00000 339007	ST	34	0.01239 059	0.13416 08	no	0.17391 3017	0.034 527	no	0.40723 5369	0.68152 0821	no	0.1360 51561
<i>GRIN1</i>	ENSP00000	Ca	18	0.00267	-	no	0.78425	-	no	0.40153	-	no	0.3624

	360608			627	0.02448 3637		3651	0.073 25		4161	0.20039 5883		22113
<i>GRIN2 A</i>	ENSP00000 332549	Ca	12	0.00018 5	- 0.01997 8253	no	0.82624 1727	0.023 598	no	0.65844 9765	- 1.09885 6784	Do wn	0.0402 89652
<i>GRIN2 C</i>	ENSP00000 293190	Ca	10	0.00008 28	- 0.06760 7325	no	0.27254 5164	0.000 465	no	0.99392 5086	- 0.03065 8879	no	0.8884 47139
<i>GRIN2 D</i>	ENSP00000 263269	Ca	10	0.00008 28	0.01764 0261	no	0.81872 1006	- 0.068 4	no	0.23157 3836	- 0.15393 082	no	0.8101 90058
<i>GRM1</i>	ENSP00000 282753	Ca	46	0.00168 435	0.02389 1092	no	0.67094 0189	- 0.231 28	Do wn	0.00788 8872	- 0.52683 163	no	0.2954 72353
<i>GRM5</i>	ENSP00000 306138	Ca	48	0.00373 03	- 0.09015 7207	no	0.10036 2644	0.117 849	Up	0.03446 0137	- 0.29059 2791	no	0.3455 08814
<i>GRPR</i>	ENSP00000 369643	Ca	42	0.00000 382	- 0.05554 4305	no	0.47408 8705	- 0.083 11	no	0.09045 6741	0.04510 1347	no	0.8359 32347
<i>GSK3 B</i>	ENSP00000 324806	ST	31	0.03985 954	- 0.56287 5324	Do wn	4.43231 E-06	- 0.182 47	Do wn	2.75596 E-10	- 0.20100 8769	no	0.5426 67881
<i>GSTP1</i>	ENSP00000 381607	CON	4	0.02033 756	- 0.81235 0991	Do wn	3.14081 E-05	- 0.236 41	Do wn	2.61693 E-06	0.54394 2919	no	0.2744 34846
<i>HAND 1</i>	ENSP00000 231121	ST	3	0.00007 25	0.07938 9499	no	0.34737 2449	0.042 779	no	0.17453 6039	- 0.26557 9967	no	0.2382 94632
<i>HDAC 1</i>	ENSP00000 362649	CON	27	0.03262 084	0.17335 5672	no	0.21343 4449	0.019 098	no	0.71099 9269	0.03820 3525	no	0.8651 72009
<i>HESX 1</i>	ENSP00000 295934	ST	1	0	0.04694 851	no	0.36173 578	0.060 553	no	0.33507 4905	0.52190 8034	no	0.2188 95253
<i>HOXB 1</i>	ENSP00000 355140	ST	2	0.00682 594	- 0.17990 224	Do wn	0.00791 1256	- 0.002 6	no	0.97030 8301	- 0.22483 583	no	0.2339 83031
<i>HRAS</i>	ENSP00000 309845	ST	37	0.01049 836	- 0.89099 2933	Do wn	2.55324 E-09	- 0.327 71	Do wn	2.43558 E-10	- 0.71109 7808	no	0.0778 84419
<i>HRH1</i>	ENSP00000 380247	Ca	43	0.00047	0.07555 4575	no	0.37426 9443	0.012 249	no	0.82734 0048	0.65735 8695	no	0.2266 40155
<i>HRH2</i>	ENSP00000 366506	Ca	21	0.00000 275	- 0.12790 8575	no	0.10141 0648	- 0.017 09	no	0.68300 89	- 0.18677 9109	no	0.3656 05641
<i>HTR2 A</i>	ENSP00000 367959	Ca	45	0.00426 483	- 0.05947 057	no	0.30275 8145	0.130 321	Up	0.00431 4674	0.03903 9577	no	0.9541 11957
<i>HTR4</i>	ENSP00000 353915	Ca	21	0.00000 275	- 0.17415 617	Do wn	0.00587 3678	- 0.079 07	no	0.08192 0506	- 0.18215 6995	no	0.3475 66203
<i>HTR6</i>	ENSP00000 289753	Ca	22	0.00057 6	- 0.07268 614	no	0.22694 529	0.027 427	no	0.61549 4184	- 0.11142 3257	no	0.6317 52012
<i>HTR7</i>	ENSP00000 337949	Ca	21	0.00000 275	- 0.12143 3044	Do wn	0.02506 5647	0.138 847	Up	0.03184 0716	- 0.49341 2135	no	0.0932 03046
<i>ID1</i>	ENSP00000 365280	ST	3	0.00017 1	- 1.20657 512	Do wn	5.70183 E-08	- 0.346 18	Do wn	1.86906 E-12	0.94674 1614	no	0.1663 37906
<i>ID2</i>	ENSP00000 234091	ST	4	0.00116 652	- 0.56693 9734	Do wn	0.00239 8096	- 0.215 76	Do wn	0.00038 6567	0.62544 8485	no	0.2625 00108
<i>ID3</i>	ENSP00000 363689	ST	2	0.00682 594	- 0.29889 7543	no	0.16355 4189	- 0.197	Do wn	0.00857 6684	0.25916 2096	no	0.6264 32588
<i>ID4</i>	ENSP00000 367972	ST	1	0	0.59155 1548	Do wn	0.01420 0785	- 0.199 02	Do wn	0.01375 6553	- 0.34963 0164	no	0.6113 94445
<i>IGF1</i>	ENSP00000 302665	CON	28	0.04312 205	- 0.05156 3378	no	0.69726 6013	- 0.047 49	no	0.43146 5367	0.28047 6932	no	0.6695 6775
<i>IGFBP 1</i>	ENSP00000 275525	ST	2	0	0.01483 7928	no	0.68326 0678	0.047 583	no	0.14714 9277	- 0.06023	no	0.8352 02534

											3499		
<i>IGFBP 2</i>	ENSP00000 233809	ST	1	0	0.03933 7636	no	0.91899 4593	0.027 73	no	0.84965 1004	0.95885 4082	no	0.2285 19244
<i>IGFBP 3</i>	ENSP00000 370473	ST	4	0.00040 7	0.13458 6986	no	0.68941 0653	0.033 758	no	0.74530 573	2.01258 2224	Up	0.0020 01928
<i>IGFBP 4</i>	ENSP00000 269593	ST	4	0.00227 551	- 0.63924 9613	Do wn	0.00077 7461	- 0.295 11	Do wn	6.12729 E-05	- 0.01371 9181	no	0.9802 4487
<i>IGFBP 5</i>	ENSP00000 233813	ST	2	0	- 0.40863 2308	no	0.12591 4093	- 0.173 95	no	0.05430 6871	0.90715 9497	no	0.2465 07093
<i>IGFBP 6</i>	ENSP00000 301464	ST	1	0	- 0.13512 7596	no	0.49825 1851	- 0.044 72	no	0.47301 9	- 0.19942 0337	no	0.7430 44626
<i>IGFBP 7</i>	ENSP00000 295666	ST	3	0.00036 9	- 0.41036 2123	no	0.07293 0625	- 0.246 46	Do wn	0.00260 6339	0.20235 2782	no	0.7765 8848
<i>ISL1</i>	ENSP00000 230658	ST	1	0	0.10279 5663	no	0.10800 9652	0.115 12	Up	0.00541 5467	- 0.63165 5977	no	0.4239 25135
<i>ITPR1</i>	ENSP00000 306253	Ca	23	0.01510 186	0.30312 0385	Up	0.04511 9675	0.339 227	Up	0.00210 8493	0.92893 3616	no	0.1193 91173
<i>ITPR2</i>	ENSP00000 370744	Ca	18	0.00867 089	- 0.06506 6639	no	0.37017 8882	- 0.187 33	Do wn	0.00038 4716	- 0.19287 095	no	0.7101 05482
<i>ITPR3</i>	ENSP00000 363435	Ca	22	0.01942 364	- 0.17880 3357	no	0.26962 3007	0.030 351	no	0.67187 5922	0.16791 1281	no	0.7425 62621
<i>JARID 2</i>	ENSP00000 341280	ST	1	0	- 0.09663 9831	no	0.45183 5097	- 0.004 31	no	0.94030 4344	- 0.04113 6497	no	0.9338 51652
<i>JUN</i>	ENSP00000 360266	CON	31	0.03792 962	- 0.73520 0966	Do wn	8.92807 E-06	- 0.120 43	no	0.17136 6276	- 0.06097 7387	no	0.9006 56682
<i>KAT2 B</i>	ENSP00000 263754	CON	18	0.00631 839	0.32267 8008	no	0.25347 3925	0.044 638	no	0.64952 4223	0.14035 1516	no	0.7297 77227
<i>KAT6 A</i>	ENSP00000 265713	ST	3	0.00000 55	0.08028 6036	no	0.40675 0049	- 0.045 08	no	0.42703 2116	0.73482 4535	no	0.1371 27411
<i>KIT</i>	ENSP00000 288135	ST	20	0.00142 449	- 1.50525 054	Do wn	8.62263 E-05	- 0.625	Do wn	8.21928 E-07	- 1.86771 7131	Do wn	0.0166 38631
<i>KLF4</i>	ENSP00000 363804	ST	8	0.00119 229	- 2.19496 5499	Do wn	1.09919 E-15	- 0.634 34	Do wn	3.76663 E-16	- 1.72802 665	Do wn	0.0015 27922
<i>LEF1</i>	ENSP00000 265165	ST	13	0.00274 525	0.26930 9477	no	0.28355 3227	0.054 432	no	0.51193 8812	1.08833 862	no	0.0595 88598
<i>LEFTY 2</i>	ENSP00000 355785	ST	2	0.00035 2	0.00399 2401	no	0.94881 0225	0.032 553	no	0.54965 2823	- 0.01315 8874	no	0.9771 99848
<i>LHCG R</i>	ENSP00000 294954	Ca	24	0.00077 5	0.01738 6812	no	0.65479 1523	0.090 285	no	0.08123 7611	- 0.00207 7043	no	0.9934 90415
<i>LIF</i>	ENSP00000 249075	ST	4	0.00031	0.44528 7786	Up	0.01453 9159	0.341 029	Up	0.00279 8926	0.40616 1416	no	0.5813 72306
<i>LIFR</i>	ENSP00000 263409	ST	4	0.00027 7	0.03909 4127	no	0.40577 9435	0.038 375	no	0.48836 1884	0.67379 2536	no	0.3868 80495
<i>LTB4R 2</i>	ENSP00000 433290	Ca	43	0.00168 384	- 0.44501 1631	Do wn	1.87791 E-05	- 0.199 05	Do wn	4.19141 E-05	- 0.37115 823	no	0.1204 65774
<i>LYN</i>	ENSP00000 428924	ST	26	0.00509 551	0.13056 2316	no	0.67144 0616	0.094 922	no	0.27570 6268	0.80885 1305	no	0.1317 19757
<i>MAOA</i>	ENSP00000 340684	CON	2	0.00682 594	- 0.39519 2052	Do wn	0.00023 0297	0.313 48	Do wn	2.39977 E-05	- 0.75622 3586	no	0.3087 84189
<i>MAP3 K1</i>	ENSP00000 382423	ST	17	0.00469 399	0.04527 6909	no	0.68847 5865	- 0.064 62	no	0.20497 2277	0.97300 1685	Up	0.0097 13086
<i>MAPK 1</i>	ENSP00000 215832	ST	42	0.05561 423	0.59174 0009	Up	0.00041 2172	0.039 168	no	0.42909 1242	- 0.21478 692	no	0.6084 60569
<i>MAPK 11</i>	ENSP00000 333685	ST	17	0.00162 874	- 0.13062 4401	Do wn	0.01599 2669	0.014 487	no	0.90517 3664	- 0.71987 1659	no	0.0558 27264

MAPK12	ENSP00000215659	ST	14	0.000758	0.074702443	no	0.643513785	0.006123	no	0.933388371	0.379637666	no	0.306037969
MAPK13	ENSP00000211287	ST	8	0.00000825	0.795184994	Down	7.35263E-10	0.44636	Down	4.3647E-12	1.276705319	no	0.097217754
MAPK14	ENSP00000229794	ST	34	0.02912488	0.054819658	no	0.605738821	0.116615	Up	0.038642425	0.336784279	no	0.358766287
MAPK3	ENSP00000263025	ST	33	0.02244545	0.299813742	Down	1.10052E-05	0.08753	Down	0.01074679	0.000265318	no	0.999319565
MEIS1	ENSP00000272369	ST	1	0	0.0003252	no	0.997341657	0.015894	no	0.682437074	0.195521186	no	0.668221819
MSC	ENSP00000321445	ST	2	0	0.44184409	Down	0.0021032	0.31033	Down	5.89108E-05	0.980688618	no	0.090754547
MYC	ENSP00000367207	ST	34	0.03598441	0.132654894	no	0.602836201	0.087	no	0.274057104	0.408910137	no	0.449615647
MYLK	ENSP00000353452	Ca	6	0.0000433	0.579985987	Down	0.002900157	0.18444	Down	0.003766651	0.782758251	no	0.237182346
NANOG	ENSP00000229307	ST	9	0.000723	0.007551062	no	0.917402394	0.05734	no	0.433134813	0.524979813	no	0.325431383
NANOGP1	ENSP00000432545	ST	1	0	no probe	no probe	no probe	no probe	no probe	no probe	no probe	no probe	no probe
NCOR1	ENSP00000268712	CON	21	0.02875081	0.059889718	no	0.627351808	0.03562	no	0.257849878	0.460598803	no	0.148831132
NEUROG1	ENSP00000317580	ST	2	0	0.145916242	Down	0.010671931	0.10119	Down	0.009517992	0.11084719	no	0.451717158
NHP2	ENSP00000274606	CON	2	0.0011897	0.076409985	no	0.511599706	0.03239	no	0.347469468	0.00238762	no	0.99490292
NODAL	ENSP00000287139	ST	6	0.00104798	0.048888979	no	0.602381853	0.11513	Up	0.023979605	0.131892887	no	0.569811133
NOS1	ENSP00000337459	Ca	32	0.01553999	0.077658425	no	0.156559391	0.11754	no	0.14979999	0.701285144	no	0.122362533
NOS2	ENSP00000327251	Ca	8	0.000749	0.148961943	Down	0.015913971	0.08347	Down	0.007454467	0.192245648	no	0.414433232
NOS3	ENSP00000297494	Ca	18	0.00431314	0.129624134	no	0.171999398	0.103497	Up	0.007516629	0.043514375	no	0.883564244
NRAS	ENSP00000358548	ST	27	0.00308327	0.802284309	Up	4.36087E-06	0.230293	Up	0.000147968	0.103512882	no	0.754482623
NTSR1	ENSP00000359532	Ca	42	0.00000382	0.012939618	no	0.845700513	0.04978	no	0.489484169	0.459394248	no	0.359347726
ONECUT1	ENSP00000302630	ST	2	0	0.003745174	no	0.962306229	0.00058	no	0.99577601	0.127167075	no	0.481234016
ORAI1	ENSP00000328216	Ca	6	0.00675581	no probe	no probe	no probe	no probe	no probe	no probe	0.209950928	no	0.573666687
ORAI2	ENSP00000348752	Ca	2	0	0.061985934	no	0.397323384	0.038541	no	0.612493991	1.418784624	no	0.085557761
ORAI3	ENSP00000322249	Ca	3	0	0.041622657	no	0.708847963	0.02418	no	0.490904569	0.339134672	no	0.314546818
OTX1	ENSP00000282549	ST	1	0	no probe	no probe	no probe	no probe	no probe	no probe	0.177142623	no	0.235525365
OXTR	ENSP00000324270	Ca	46	0.00449222	0.00710418	no	0.929951657	0.007858	no	0.822896304	0.244700775	no	0.492795142
P2RX1	ENSP00000	Ca	1	0	-	no	0.36165	0.058	no	0.08216	-	no	0.6512

	225538				0.06674 7191		847	28		0849	0.15859 24		679
P2RX2	ENSP00000 343339	Ca	3	0.01362 85	- 0.06960 9197	no	0.29464 9184	- 0.009 56	no	0.81839 6972	- 0.43346 7644	Do wn	0.0423 20371
P2RX3	ENSP00000 263314	Ca	1	0	- 0.01607 5485	no	0.76627 0034	0.097 248	no	0.05713 9593	- 0.03548 392	no	0.8416 40553
P2RX4	ENSP00000 336607	Ca	1	0	0.41272 6095	Up	0.00513 1297	0.096 306	Up	0.00916 174	0.23700 254	no	0.6094 47321
P2RX6	ENSP00000 416193	Ca	1	0	- 0.11402 5437	no	0.08018 3886	0.145 606	Up	0.00020 5534	- 0.07784 63	no	0.7219 10798
P2RX7	ENSP00000 442349	Ca	1	0	- 0.55689 8902	Do wn	0.00957 0002	- 0.087 05	no	0.07713 4747	- 0.01376 1729	no	0.9858 12605
PAX6	ENSP00000 368401	ST	7	0.01430 283	- 0.02363 7145	no	0.81580 7945	0.044 49	no	0.55575 3933	- 0.12345 8766	no	0.8321 31827
PDGF RA	ENSP00000 257290	Ca	19	0.00114 609	- 0.79923 5614	Do wn	0.00070 2045	- 0.026 33	no	0.62910 7468	0.68820 6632	no	0.2552 63685
PDGF RB	ENSP00000 261799	Ca	24	0.00281 377	- 0.57269 4082	Do wn	9.96889 E-05	- 0.326 33	Do wn	1.79765 E-06	0.06683 2333	no	0.8986 23877
PHKG 1	ENSP00000 297373	Ca	2	0	0.08593 137	no	0.21080 6349	0.051 23	no	0.14688 9631	- 0.08088 1259	no	0.6398 21948
PIK3C G	ENSP00000 352121	ST	35	0.00535 44	0.13165 9975	no	0.12793 4481	- 0.112 71	no	0.21198 8872	0.32361 2116	no	0.6272 7963
PIK3R 1	ENSP00000 274335	ST	69	0.05441 236	- 0.17601 4314	no	0.38390 6559	- 0.120 78	Do wn	0.03005 9149	0.83403 2706	no	0.0578 25554
PIK3R 5	ENSP00000 392812	ST	33	0.00494 904	- 0.02552 5624	no	0.71939 2022	0.003 78	no	0.90171 9996	- 0.81381 1885	no	0.1038 1709
PLCB 1	ENSP00000 338185	Ca	68	0.01829 564	0.08730 6204	no	0.33755 2618	0.109 468	no	0.15959 6073	- 0.49289 5971	no	0.4448 77184
PLCB 2	ENSP00000 260402	Ca	66	0.01380 784	- 0.04727 4128	no	0.50917 8203	- 0.092 86	no	0.10972 8175	- 0.06079 8796	no	0.8939 80024
PLCB 3	ENSP00000 279230	Ca	66	0.01380 784	0.33340 2195	Do wn	2.05604 E-05	0.009 61	no	0.85044 9402	- 0.48136 8338	Do wn	0.0203 0294
PLCB 4	ENSP00000 334105	Ca	66	0.01320 147	0.10959 2421	no	0.38408 0228	0.079 701	no	0.45208 2054	0.12329 0515	no	0.9235 4817
PLCD 1	ENSP00000 430344	Ca	18	0.00032 6	0.32014 3416	Do wn	8.46033 E-08	0.064 17	no	0.16964 6016	- 0.63516 2508	no	0.1087 59044
PLCD 3	ENSP00000 313731	Ca	17	0.00015 3	<i>no probe</i>	<i>no probe</i>	<i>no probe</i>	<i>no probe</i>	<i>no probe</i>	<i>no probe</i>	- 0.61267 7715	Do wn	0.0049 68125
PLCD 4	ENSP00000 388631	Ca	17	0.00015 3	<i>no probe</i>	<i>no probe</i>	<i>no probe</i>	<i>no probe</i>	<i>no probe</i>	<i>no probe</i>	- 1.15137 6888	Do wn	0.0162 22404
PLCE 1	ENSP00000 260766	Ca	21	0.00052 6	0.00408 4141	no	0.95854 1755	0.041 715	no	0.47545 8787	0.89882 3901	no	0.1785 37484
PLCG 1	ENSP00000 244007	Ca	49	0.01645 968	0.03496 9043	no	0.74740 5232	0.036 399	no	0.38789 858	0.55545 2063	Up	0.0246 80198
PLN	ENSP00000 350132	Ca	4	0.00144 688	- 0.04795 8773	no	0.74195 927	0.020 75	no	0.80121 0628	0.79537 2779	no	0.2955 86562
POU5 F1	ENSP00000 259915	ST	7	0.00066	<i>no probe</i>	<i>no probe</i>	<i>no probe</i>	<i>no probe</i>	<i>no probe</i>	<i>no probe</i>	<i>no probe</i>	<i>no probe</i>	<i>no probe</i>
PPIF	ENSP00000 225174	Ca	6	0.01127 904	0.19187 3255	no	0.19821 0866	0.082 622	no	0.21341 6041	0.73157 6058	no	0.1974 84379
PPP1 CC	ENSP00000 335084	CON	22	0.01965 509	0.60974 7304	Up	1.52233 E-05	0.157 544	Up	3.22551 E-05	0.16737 5812	no	0.3079 97432

PRC1	ENSP00000 377793	ST	3	0	0.60500 5497	Up	0.00429 5023	0.142 992	Up	0.00929 3472	0.13587 168	no	0.7285 06463
PRKACA	ENSP00000 309591	CON	51	0.08370 37	- 0.22973 9375	Down	0.00193 898	0.102 36	Down	0.00616 6758	0.57794 4363	no	0.0569 47292
PRKCA	ENSP00000 408695	Ca	55	0.03906 664	0.47690 2328	Up	0.00386 0994	0.096 9	no	0.22782 6787	- 0.04876 9984	no	0.9342 20679
PRKCB	ENSP00000 305355	Ca	44	0.01690 36	0.32258 8256	no	0.31427 1066	0.030 37	no	0.60095 4741	0.28691 6522	no	0.7548 43222
PRKCG	ENSP00000 263431	Ca	35	0.00716 81	- 0.11104 8826	no	0.10202 9504	0.080 34	no	0.23839 8963	- 0.16591 8417	no	0.3551 09799
PROM1	ENSP00000 415481	ST	1	0	0.06027 3534	no	0.31518 0126	0.094 452	Up	0.01504 0622	0.26297 1426	no	0.7832 6559
PTAFR	ENSP00000 301974	Ca	43	0.00208 304	- 0.01167 5406	no	0.92545 7757	0.161 96	Down	0.01231 2197	- 0.30352 8499	no	0.5423 61345
PTEN	ENSP00000 361021	ST	22	0.00613 556	0.37856 366	Up	0.00400 0411	0.074 292	no	0.23554 371	- 0.07631 7161	no	0.8651 82847
PTGER1	ENSP00000 292513	Ca	45	0.00048 5	- 0.21654 5773	Down	0.00006 3034	0.066 08	no	0.47658 7127	- 0.22006 7713	no	0.3390 85974
PTGER3	ENSP00000 349003	Ca	15	0.00027 9	- 0.01796 286	no	0.79478 9452	0.214 549	Up	0.00112 0931	- 1.46589 8247	Down	0.0428 34648
PTGFR	ENSP00000 359793	Ca	42	0.00000 382	- 0.17343 7897	Down	0.01162 1634	0.090 78	Down	0.04937 4287	- 0.73421 2216	no	0.1044 75344
PTK2B	ENSP00000 332816	Ca	20	0.00295 102	- 0.30556 3784	Down	0.01175 0578	0.142 36	Down	0.01019 8577	- 0.34433 873	no	0.3854 06587
PTPN11	ENSP00000 340944	ST	34	0.02374 219	0.34858 8259	Up	0.03990 8343	0.147 05	Up	0.00909 2992	1.20793 6326	Up	0.0482 64037
RAF1	ENSP00000 251849	ST	27	0.01186 176	0.12277 2265	no	0.24864 1936	0.079 43	Down	0.00124 894	0.55979 0317	no	0.1831 38052
REST	ENSP00000 311816	ST	2	0	- 0.09758 1434	no	0.24349 7937	0.254 397	Up	0.00031 0556	1.00959 4871	Up	0.0241 98881
RIF1	ENSP00000 243326	ST	1	0	- 0.00339 7582	no	0.94211 2086	0.033 43	no	0.68804 4015	1.50065 0292	Up	0.0380 49024
RRAS	ENSP00000 246792	ST	12	0.00028 2	- 0.37763 3449	Down	0.00060 3199	0.165 25	Down	5.35327 E-05	- 0.48276 9566	no	0.2893 82644
RYR1	ENSP00000 352608	Ca	7	0.00069 9	0.46944 6952	Down	0.01358 497	0.004 308	no	0.94802 7757	0.26275 6533	no	0.7331 36393
RYR2	ENSP00000 355533	Ca	10	0.00095 9	- 0.07644 8117	no	0.15283 9664	0.217 964	Up	0.00023 1604	- 0.34769 0769	no	0.6684 23945
RYR3	ENSP00000 373884	Ca	4	0.00009 05	0.04293 1871	no	0.34021 0558	0.016 311	no	0.60149 7128	- 1.04579 4583	Down	0.0350 7429
SALL4	ENSP00000 217086	CON	10	0.00803 744	<i>no probe</i>	<i>no probe</i>	<i>no probe</i>	<i>no probe</i>	<i>no probe</i>	<i>no probe</i>	0.41497 2234	no	0.3107 25094
SDCI	ENSP00000 254351	CON	7	0.00959 994	- 1.51784 1904	Down	3.24338 E-08	0.885 33	Down	1.98433 E-18	- 1.20981 7907	no	0.1207 51119
SETDB1	ENSP00000 271640	ST	4	0.00687 492	- 0.08288 6696	no	0.38879 0347	0.002 68	no	0.95676 2155	0.34701 7789	no	0.3322 9295
SKIL	ENSP00000 259119	ST	7	0.00007 62	0.08020 6068	no	0.18497 4683	0.243 431	Up	0.00096 1394	1.21752 3077	Up	0.0421 11939
SLC25A4	ENSP00000 281456	Ca	4	0	- 0.07055 5962	no	0.75860 5509	0.035 86	no	0.50929 3775	- 0.17352 2016	no	0.7533 28025
SMAD2	ENSP00000 262160	ST	29	0.02336 588	0.21066 2187	Up	0.00946 6433	- 0.005	no	0.92471 9732	- 0.35259	no	0.2329 6179

								93			4394		
SMAD3	ENSP00000332973	ST	28	0.02392531	0.004737328	no	0.975647588	0.107429	no	0.09794078	-0.389901573	no	0.219862918
SMAD4	ENSP00000341551	ST	35	0.03753624	0.791374313	Up	5.56315E-06	0.169068	Up	0.000292094	0.767650726	no	0.141417242
SMAD6	ENSP00000288840	ST	11	0.0000636	-0.175308617	Down	0.003524164	-0.20426	Down	0.011566706	-0.258314473	no	0.613723435
SMAD7	ENSP00000262158	ST	23	0.01209405	-0.028194174	no	0.804157049	-0.08113	no	0.091548427	0.276889098	no	0.475879695
SMARCAD1	ENSP00000351947	ST	1	0	no probe	no probe	no probe	no probe	no probe	no probe	0.44053724	no	0.106229561
SOX10	ENSP00000354130	CON	4	0.00714344	0.105632401	no	0.746567393	0.004321	no	0.970404437	0.471768938	no	0.465272466
SOX2	ENSP00000323588	ST	11	0.00285805	-0.026059678	no	0.758192096	0.13704	no	0.055856357	-1.424207065	no	0.205219819
SPHK1	ENSP00000313681	Ca	8	0.000928	0.332048987	Up	0.022055475	0.06938	no	0.192485996	0.666475986	no	0.200180758
STAT3	ENSP00000264657	ST	28	0.0154567	-0.028899098	no	0.834520123	-0.09668	no	0.054324093	0.783935787	no	0.058644045
STIM1	ENSP00000300737	Ca	7	0.01353499	-0.244653986	Down	0.000488812	-0.03882	no	0.202125033	0.161127766	no	0.695734504
STIM2	ENSP00000417569	Ca	4	0.0000234	no probe	no probe	no probe	no probe	no probe	no probe	0.690876505	no	0.141103889
TACR1	ENSP00000303522	Ca	42	0.00000382	-0.126076241	no	0.124287544	-0.07838	no	0.140929089	-1.607489836	Down	0.006947436
TACR2	ENSP00000362403	Ca	42	0.00000382	-0.093732789	no	0.188585427	0.061091	no	0.208532278	0.25173582	no	0.46233114
TACR3	ENSP00000303325	Ca	42	0.00000382	0.094073756	no	0.196294259	0.037577	no	0.206309235	-0.01905164	no	0.902123229
TBX3	ENSP00000257566	ST	1	0	0.15667443	no	0.230868791	0.087755	no	0.46113262	1.014261146	no	0.09093181
TBXA2R	ENSP00000393333	Ca	47	0.00301697	-0.094549545	no	0.142307589	0.118784	Up	0.003640564	0.366669553	no	0.544911813
TCF3	ENSP00000262965	ST	18	0.02573384	0.030892143	no	0.803481248	0.118718	no	0.217139092	0.388196991	no	0.260191349
THY1	ENSP00000284240	ST	1	0	0.473451414	Down	0.000382645	-0.25112	Down	9.17744E-05	-0.097689432	no	0.867512422
TLE4	ENSP00000365735	CON	5	0.00682854	0.130596856	no	0.449657637	0.017118	no	0.852363111	0.112191689	no	0.875586586
TRHR	ENSP00000309818	Ca	42	0.00000382	0.139025291	Up	0.04514731	0.110461	Up	0.000240935	-0.140199544	no	0.44240227
VDAC1	ENSP00000265333	Ca	7	0.01610604	0.314250026	Up	0.018856803	-0.00427	no	0.946198996	0.924120346	no	0.092489525
VDAC2	ENSP00000361635	Ca	4	0	0.100897002	no	0.478050986	0.02276	no	0.620516463	-0.278891688	no	0.143231604
VDAC3	ENSP00000428845	Ca	5	0.00682594	0.122150714	no	0.313363466	0.040102	no	0.305878668	1.002343479	no	0.060285107
WNT1	ENSP00000293549	ST	33	0.01609896	-0.004445517	no	0.947027658	0.05291	no	0.138904226	-0.146432726	no	0.420289685
WNT10A	ENSP00000258411	ST	27	0.0000201	no probe	no probe	no probe	no probe	no probe	no probe	-1.051014506	Down	0.006104193
WNT1	ENSP00000	ST	28	0.00423	-	no	0.54975	-	no	0.17291	-	no	0.2164

OB	301061			025	0.06527 3366		1248	0.102 01		3743	0.45959 241		14778
WNT1 I	ENSP00000 325526	ST	27	0.00002 01	- 0.19877 9226	Do wn	0.00223 7576	- 0.160 37	Do wn	0.02908 149	- 0.60112 241	no	0.1265 76731
WNT1 6	ENSP00000 222462	ST	27	0.00002 01	0.01744 3978	no	0.79630 8339	0.057 444	no	0.23734 5562	- 2.13889 0939	Do wn	0.0149 76208
WNT2	ENSP00000 265441	ST	28	0.00077 4	0.14920 1682	no	0.07729 9817	0.103 869	Up	0.00850 0292	- 0.20696 4908	no	0.6597 177
WNT2 B	ENSP00000 358698	ST	27	0.00002 01	- 0.05721 198	no	0.39377 9725	0.012 966	no	0.79800 7509	- 0.29092 1771	no	0.4047 09278
WNT3	ENSP00000 225512	ST	27	0.00002 01	- 0.34589 1879	Do wn	9.14835 E-07	- 0.085 56	Do wn	0.00537 9583	- 0.62360 6598	no	0.3563 00932
WNT3 A	ENSP00000 284523	ST	33	0.01580 006	<i>no probe</i>	<i>no probe</i>	<i>no probe</i>	<i>no probe</i>	<i>no probe</i>	<i>no probe</i>	<i>no probe</i>	<i>no probe</i>	<i>no probe</i>
WNT4	ENSP00000 290167	ST	27	0.00002 01	- 1.03378 4268	Do wn	1.73126 E-15	- 0.408 09	Do wn	7.82447 E-15	- 1.47788 7308	Do wn	0.0177 02159
WNT5 A	ENSP00000 264634	ST	29	0.00866 196	- 0.62506 5857	Do wn	2.03354 E-06	- 0.228 63	Do wn	4.43848 E-06	- 1.66925 5786	Do wn	0.0017 85341
WNT5 B	ENSP00000 308887	ST	27	0.00002 01	- 0.19662 1821	Do wn	0.01713 064	- 0.109 38	no	0.05840 3641	- 0.77866 6315	no	0.1165 73098
WNT6	ENSP00000 233948	ST	27	0.00002 01	0.08957 4217	no	0.32399 6843	- 0.094 6	Do wn	0.03067 9811	- 0.59501 5336	no	0.1286 00012
WNT7 A	ENSP00000 285018	ST	28	0.00077 4	0.07991 7014	no	0.11679 2267	- 0.019 28	no	0.68929 0889	- 0.35579 0357	no	0.1050 68669
WNT7 B	ENSP00000 341032	ST	27	0.00002 01	- 0.31256 1559	Do wn	4.87495 E-06	- 0.195 48	Do wn	5.79645 E-06	- 0.46383 41	Do wn	0.0331 64429
WNT8 A	ENSP00000 381739	ST	30	0.00310 753	<i>no probe</i>	<i>no probe</i>	<i>no probe</i>	<i>no probe</i>	<i>no probe</i>	<i>no probe</i>	- 0.19547 4245	no	0.3140 72573
WNT8 B	ENSP00000 340677	ST	30	0.00310 753	0.11899 919	no	0.08635 3151	- 0.018 3	no	0.77882 8694	- 0.07904 5592	no	0.6858 34465
WNT9 A	ENSP00000 272164	ST	27	0.00002 01	<i>no probe</i>	<i>no probe</i>	<i>no probe</i>	<i>no probe</i>	<i>no probe</i>	<i>no probe</i>	- 0.79681 0057	Do wn	0.0172 24254
WNT9 B	ENSP00000 290015	ST	27	0.00002 01	<i>no probe</i>	<i>no probe</i>	<i>no probe</i>	<i>no probe</i>	<i>no probe</i>	<i>no probe</i>	- 0.06612 0029	no	0.6969 58394
ZIC3	ENSP00000 287538	ST	5	0	0.12027 8857	no	0.06559 5744	0.151 457	Up	0.00949 0133	- 0.21748 7605	no	0.2032 26624
ZNF59 3	ENSP00000 363384	ST	2	0.00016 4	- 0.08258 3463	no	0.60832 8638	0.001 154	no	0.98499 5034	0.42242 9503	no	0.4416 91105

3. Discussão dos Resultados

No artigo do presente trabalho, apresentamos a montagem de um grafo modelando a interação entre proteínas membros da integração das vias de sinalização do íon cálcio e da regulação da pluripotência de células tronco. A rede apresenta alta densidade: 2995 interações para 294 proteínas, com valor de enriquecimento de interações significativo (teste hipergeométrico com $p < 0,001$). Isso indica que essas proteínas tem maior grau de conectividade do que esperado ao acaso para um conjunto de nós do mesmo tamanho e isso, por consequência, sugere uma ligação biológica modular entre elas. Esse resultado corrobora com o fato de que as proteínas vieram de anotações de vias anotadas pelo KEGG, portanto se espera que sejam funcionalmente ligadas em nível de interatoma. O algoritmo proposto conectou as proteínas de ambas as vias analisadas sem perder o enriquecimento significativo de interações e gerando um modelo *in silico* robusto. Além disso, embora o limiar para o escore de confiança das interações tenha sido de 0,400 (de média confiança), os escores das interações de toda a rede apresentam média $> 0,864$ (alta confiança), reforçando a robustez deste modelo. Por fim, a rede segue uma distribuição de graus livre de escala com α igual a aproximadamente 7 (teste de Kolmogorov-Smirnov com valor $p > 0,05$, rejeitando a hipótese de que a distribuição de graus não segue uma lei exponencial). Isso mais uma vez reforça a validade do modelo, pois sabe-se que grafos oriundos de redes biológicas têm como propriedade quase universal a distribuição livre de escala (JEONG *et. al.*, 2000). Este modelo recebeu o nome de *STEMCa* e será referenciado assim daqui adiante no texto.

Em uma segunda etapa, utilizamos experimentos independentes de grupos de pacientes com melanoma, para os quais foram feitas biópsias de tumores primários ou metastáticos, e essas amostras foram submetidas a semi-quantificação da expressão gênica por microarranjo. Esses dados foram utilizados para análise de expressão diferencial, a qual

apontou que mais de 50% (151 de 294) dos genes que codificam as proteínas membros do modelo *STEMCa* estão diferencialmente expressos (valor p corrigido por FDR < 0.05) em pelo menos um dos experimentos avaliados. Isso sugere que, a nível transcricional, a integração das vias de sinalização do cálcio e regulação da pluripotência de células tronco está desregulada nas células com poder de metástase. Dentre os 151 genes diferencialmente expressos, 64 pertencem à via de sinalização do cálcio, enquanto 75 pertencem à via de regulação da pluripotência de células tronco, portanto são ambas as vias que contribuem para a expressão aberrante no modelo “STEMCa”. Além disso, o algoritmo utilizado para montagem e integração da rede adicionou 21 nós (proteínas) não anotadas pelo KEGG como pertencentes à nenhuma das vias avaliadas, os quais são chamados nesse trabalho de *conectores*. Dos 21 *conectores* adicionados ao modelo “STEMCa”, 11 estão diferencialmente expressos, dentre os quais 7 ocupam posições centrais no interatoma (alto grau e/ou alto *betweenness*). Isso sugere que a integração dos *conectores* é funcional (com significado biológico) e não ao acaso, pois eles contribuem tanto para o perfil modular do interatoma (*i.e.* sua remoção levaria ao colapso da rede) quanto para a expressão desregulada de ambas as vias estudadas.

Contudo, a análise de expressão diferencial limita-se à avaliação individual do status de cada gene (super ou subexpresso), ao passo que nosso estudo busca também a avaliação da expressão gênica em metástase de melanomas para o modelo “STEMCa” como um conjunto modular único. Para atingir esse objetivo, utilizamos a ferramenta *GALANT*, a qual plota perfis de expressão gênica sobre redes de interação proteica com base no *log Fold Change* dos genes codificadores das proteínas que compõe a rede estudada. Com o resultado apresentado na figura 2 do artigo, fica evidente a similaridade consistente entre os perfis de expressão do modelo “STEMCa” nos 3 conjuntos de dados independentes que foram avaliados.

Por fim, os cálculos topológicos feitos sob a rede apontam as proteínas *CTNNB1*, *GNAQ*, *GSK3B*, *GSTP1*, *MAPK3*, *PPP1CC*, *PRKACA*, *SMAD4*, e *PTPN11* como aquelas que têm posição central no interatoma e ao mesmo tempo se apresentam diferencialmente expressas. Ou seja, esse subconjunto de proteínas do modelo “STEMCa” exerce forte influência dentro interatoma por conta de suas propriedades topológicas e, portanto, tendo a expressão de seus genes codificadores desregulada, deverão influenciar no funcionamento modular da rede como um todo (análogo a se estragar uma peça fundamental dentro de um motor, levando-o ao mal funcionamento). Por essa razão, essas proteínas centrais são aqui sugeridas como potenciais candidados de um grupo biomarcador de metástase em melanomas, assim como possíveis alvos terapêuticos.

A detecção de metástases nos estágios iniciais é difícil e, por isso, a migração de células tumorais para tecidos além do sítio do tumor representa mais de 90% das mortes causadas por câncer (Chambers *et al.*, 2002). Sendo assim, a elucidação das vias que atuam na promoção de metástase e a exploração de novos biomarcadores que contribuam para a detecção precoce de uma neoplasia potencialmente maligna são de grande relevância.

Nosso modelo “STEMCa” busca modelar a integração das vias de regulação do íon cálcio e da regulação da plitipotência de CTs. Sabe-se que as CTs e as CTTs dividem características similares em nível celular (potência e auto-renovação) e molecular (expressão de marcadores como, por exemplo, proteínas de superfície e biomarcadores de pluripotência) (Oren e Smith, 2016). As CTTs, por sua vez, apresentam características importantes para promover metástase em câncer, já que possuem o poder de auto-renovação e também podem dar origem às demais células que compõe a população heterogênea do tumor. A literatura científica é vasta de exemplos demonstrando que células de um tumor que expressam marcadores de tronco tendem a ser mais invasivas e, mesmo em pequena quantidade, são capazes de repopular todo o sítio tumoral, restaurando o câncer (Jordan e Guzman, 2004;

Singh, Clarke, *et al.*, 2004; Valk-Lingbeek *et al.*, 2004). O segundo componente do modelo “STEMCa” refere-se à sinalização dependente do íon cálcio, a qual tem papel fundamental na proliferação e diferenciação celular em CTs no estágio embrionário (Carafoli e Krebs, 2016). Apesar da falta de estudos detalhados das vias de sinalização de Ca^{2+} em CTs pluripotentes, nós especulamos que a atividade transcricional de ambos componentes do modelo “STEMCa” pudessem contribuir para a promoção de metástase em melanomas. Nossos resultados sugerem que essa hipótese é válida, embora estudos seguintes sejam necessários para confirmação destes dados em nível proteico.

Outro processo que parece relevante para a progressão de metástases é a transição epitélio-mesenquimal (TEM), que embora tenha papel fundamental no desenvolvimento da mesoderme nos estágios de desenvolvimento embrionário, também é reconhecida como um mecanismo patológico no surgimento de várias doenças, incluindo fibrose e câncer (Gos *et al.*, 2009). Sabe-se que durante a TEM, uma célula com atributos fenotípicos de células epiteliais sofre uma radical reprogramação celular, passando a ter atributos de células mesenquimais (*i.e.* tornam-se móveis e capazes de invadir a matriz extra-celular), ou seja, potencialmente mais invasivas (Lee *et al.*, 2006). No modelo *STEMCa* temos um clique de proteínas da via de sinalização *Wnt* com expressão aberrante, para qual estudos sugerem que sua ativação contribui para a indução e manutenção de CTTs ativadas por TEM (Scheel *et al.*, 2011). Apresentamos ainda *CTNNB1* como um dos nós centrais da rede, uma proteína que provê o recrutamento de fatores de transcrição ativados pela via de sinalização *Wnt* (Chang *et al.*, 2015). Além disso, observamos *GSK3B* (cinase que reprime a via de sinalização *Wnt*, fosforilando *CTNNB* e, assim, marcando-a para degradação) como um nó gargalo e significativamente subexpresso em 2 das 3 côrtes avaliadas.

As fosfatases têm poder de controlar amplitude e intensidade de sinais de cascatas de fosforilação, que exercem papel fundamental em muitos processos biológicos, dentre os

quais está o comprometimento entre proliferação/diferenciação (Tonks, 2013). Com isso, apontamos outra proteína pertencente ao grupo central do modelo *STEMCa*: a PPP1CC, que pertence à família de fosfatases, subfamília PP1. Takarura *et al.* avaliou sistematicamente o papel de 9 fosfatases da família PP1 (incluindo PPP1CC) em 55 linhagens celulares de cânceres humanos, abrangendo pulmão, coloretal, gástrico e ovário (Takakura *et al.*, 2001). Apesar da expressão constitutiva de muitos dos genes avaliados em todas as linhagens, foram observadas alterações pontuais de expressão diferencial e mutações somáticas e/ou polimorfismos câncer-específicos em membros da família PP1, indicando seu envolvimento na carcinogênese. Além disso, PPP1CC já foi reportada em outro modelo de interação proteína-proteína como um nó central em câncer coloretal (Kou *et al.*, 2015), tendo sido este modelo criado a partir de genes desregulados em amostras de biópsia de tumores em comparação a tecidos saudáveis. Em especial, no entanto, apontamos a fosfatase PTPN11, da família de proteínas tirosina-fosfatases, como a única que mostrou constitutivamente superexpressão nos 3 conjuntos de dados independentes avaliados. Estudos mostram que a inibição de PTPN11 impede a aquisição de quimioresistência a drogas que funcionam ativando receptores de tirosina cinase. Sabendo-se que as CTTs apresentam quimioresistência, a superexpressão consistente de PTPN11 e sua centralidade no modelo “STEMCa” sugerem esse gene/proteína como um biomarcador interessante a ser investigado.

Por último, conclui-se nesse trabalho:

1. Obtivemos um modelo de interação proteína-proteína robusto da integração da via de sinalização do íon cálcio e regulação da pluripotência de CTs.
2. Observamos um padrão consistente de expressão anormal do perfil transcricional dos genes codificadores das proteínas membro do modelo

proposto ao se comparar tumores primários e metastáticos de melanoma humano.

3. Identificamos e propomos, através da combinação de cálculos topológicos e expressão diferencial, um conjunto de genes biomarcadores de metástase em melanoma humano, com destaque à fosfatase PTPN11.

4. Referências Bibliográficas

AL-HAJJ, M. et al. Prospective identification of tumorigenic breast cancer cells. **Proc Natl Acad Sci U S A**, v. 100, n. 7, p. 3983-8, Apr 1 2003. ISSN 0027-8424 (Print)

0027-8424.

ALLAN, A. L. et al. Tumor dormancy and cancer stem cells: implications for the biology and treatment of breast cancer metastasis. **Breast Dis**, v. 26, p. 87-98, 2006. ISSN 0888-6008 (Print)

0888-6008.

BERRIDGE, M. J.; BOOTMAN, M. D.; RODERICK, H. L. Calcium signalling: dynamics, homeostasis and remodelling. **Nat Rev Mol Cell Biol**, v. 4, n. 7, p. 517-29, Jul 2003. ISSN 1471-0072 (Print)

1471-0072.

BRACK, A. S.; RANDO, T. A. Tissue-specific stem cells: lessons from the skeletal muscle satellite cell. **Cell Stem Cell**, v. 10, n. 5, p. 504-14, May 4 2012. ISSN 1875-9777.

CARAFOLI, E.; KREBS, J. Why Calcium? How Calcium Became the Best Communicator. **J Biol Chem**, v. 291, n. 40, p. 20849-20857, Sep 30 2016. ISSN 0021-9258 (Print)

0021-9258.

CHAMBERS, A. F.; GROOM, A. C.; MACDONALD, I. C. Dissemination and growth of cancer cells in metastatic sites. **Nat Rev Cancer**, v. 2, n. 8, p. 563-72, Aug 2002. ISSN 1474-175X (Print)

1474-175x.

CHANG, Y. W. et al. Diverse Targets of beta-Catenin during the Epithelial-Mesenchymal Transition Define Cancer Stem Cells and Predict Disease Relapse. **Cancer Res**, v. 75, n. 16, p. 3398-410, Aug 15 2015. ISSN 0008-5472.

CHARAFE-JAUFFRET, E. et al. Aldehyde dehydrogenase 1-positive cancer stem cells mediate metastasis and poor clinical outcome in inflammatory breast cancer. **Clin Cancer Res**, v. 16, n. 1, p. 45-55, Jan 1 2010. ISSN 1078-0432 (Print)

1078-0432.

CLAPHAM, D. E. Calcium signaling. **Cell**, v. 131, n. 6, p. 1047-58, Dec 14 2007. ISSN 0092-8674 (Print)

0092-8674.

CROKER, A. K. et al. High aldehyde dehydrogenase and expression of cancer stem cell markers selects for breast cancer cells with enhanced malignant and metastatic ability. **J Cell Mol Med**, v. 13, n. 8b, p. 2236-52, Aug 2009. ISSN 1582-1838.

DATTA, M. et al. Serum calcium, albumin and tumor stage in cutaneous malignant melanoma. **Future Oncol**, v. 12, n. 19, p. 2205-14, Oct 2016. ISSN 1479-6694 (Print)
1479-6694.

DREESEN, O.; BRIVANLOU, A. H. Signaling pathways in cancer and embryonic stem cells. **Stem Cell Rev**, v. 3, n. 1, p. 7-17, Jan 2007. ISSN 1550-8943 (Print)
1550-8943.

ERAMO, A. et al. Identification and expansion of the tumorigenic lung cancer stem cell population. **Cell Death Differ**, v. 15, n. 3, p. 504-14, Mar 2008. ISSN 1350-9047 (Print)
1350-9047.

FURTH, J.; KAHN, M. C. The Transmission of Leukemia of Mice with a Single Cell. **Am. J. Cancer**, v. 31, 1937 1937.

GOS, M.; MILOSZEWSKA, J.; PRZYBYSZEWSKA, M. [Epithelial-mesenchymal transition in cancer progression]. **Postepy Biochem**, v. 55, n. 2, p. 121-8, 2009. ISSN 0032-5422 (Print)
0032-5422.

HE, Y. C. et al. Apoptotic death of cancer stem cells for cancer therapy. **Int J Mol Sci**, v. 15, n. 5, p. 8335-51, May 12 2014. ISSN 1422-0067.

JORDAN, C. T.; GUZMAN, M. L. Mechanisms controlling pathogenesis and survival of leukemic stem cells. **Oncogene**, v. 23, n. 43, p. 7178-87, Sep 20 2004. ISSN 0950-9232 (Print)
0950-9232.

KAI, M. et al. Semi-quantitative evaluation of CD44(+) /CD24(-) tumor cell distribution in breast cancer tissue using a newly developed fluorescence immunohistochemical staining method. **Cancer Sci**, v. 102, n. 12, p. 2132-8, Dec 2011. ISSN 1347-9032.

KOREN, E.; FUCHS, Y. The bad seed: Cancer stem cells in tumor development and resistance. **Drug Resist Updat**, v. 28, p. 1-12, Sep 2016. ISSN 1368-7646.

KOU, Y. et al. Gene expression profile analysis of colorectal cancer to investigate potential mechanisms using bioinformatics. **Onco Targets Ther**, v. 8, p. 745-52, 2015. ISSN 1178-6930.

KOZOVSKA, Z.; GABRISOVA, V.; KUCEROVA, L. Malignant melanoma: diagnosis, treatment and cancer stem cells. **Neoplasma**, v. 63, n. 4, p. 510-7, 2016. ISSN 0028-2685 (Print)

0028-2685.

LAPIDOT, T. et al. A cell initiating human acute myeloid leukaemia after transplantation into SCID mice. **Nature**, v. 367, n. 6464, p. 645-8, Feb 17 1994. ISSN 0028-0836 (Print)

0028-0836.

LEE, J. M. et al. The epithelial-mesenchymal transition: new insights in signaling, development, and disease. **J Cell Biol**, v. 172, n. 7, p. 973-81, Mar 27 2006. ISSN 0021-9525 (Print)

0021-9525.

LI, F. et al. Beyond tumorigenesis: cancer stem cells in metastasis. **Cell Res**, v. 17, n. 1, p. 3-14, Jan 2007. ISSN 1001-0602.

MAIQUES, O. et al. Immunohistochemical analysis of T-type calcium channels in acquired melanocytic nevi and melanoma. **Br J Dermatol**, Oct 8 2016. ISSN 0007-0963.

OREN, O.; SMITH, B. D. Eliminating Cancer Stem Cells by Targeting Embryonic Signaling Pathways. **Stem Cell Rev**, Oct 11 2016. ISSN 1550-8943.

PARK, I. H. et al. Generation of human-induced pluripotent stem cells. **Nat Protoc**, v. 3, n. 7, p. 1180-6, 2008. ISSN 1750-2799.

SCHATTON, T. et al. Identification of cells initiating human melanomas. **Nature**, v. 451, n. 7176, p. 345-9, Jan 17 2008. ISSN 0028-0836.

SCHEEL, C. et al. Paracrine and autocrine signals induce and maintain mesenchymal and stem cell states in the breast. **Cell**, v. 145, n. 6, p. 926-40, Jun 10 2011. ISSN 0092-8674.

SINGH, S. K. et al. Cancer stem cells in nervous system tumors. **Oncogene**, v. 23, n. 43, p. 7267-73, Sep 20 2004. ISSN 0950-9232 (Print)

0950-9232.

SINGH, S. K. et al. Identification of human brain tumour initiating cells. **Nature**, v. 432, n. 7015, p. 396-401, Nov 18 2004. ISSN 0028-0836.

TAKAKURA, S. et al. Genetic alterations and expression of the protein phosphatase 1 genes in human cancers. **Int J Oncol**, v. 18, n. 4, p. 817-24, Apr 2001. ISSN 1019-6439 (Print)

1019-6439.

TONKS, N. K. Protein tyrosine phosphatases--from housekeeping enzymes to master regulators of signal transduction. **Febs j**, v. 280, n. 2, p. 346-78, Jan 2013. ISSN 1742-464x.

TSAI, F. C. et al. Ca²⁺ signaling in cytoskeletal reorganization, cell migration, and cancer metastasis. **Biomed Res Int**, v. 2015, p. 409245, 2015.

VALK-LINGBEEK, M. E.; BRUGGEMAN, S. W.; VAN LOHUIZEN, M. Stem cells and cancer; the polycomb connection. **Cell**, v. 118, n. 4, p. 409-18, Aug 20 2004. ISSN 0092-8674 (Print)

0092-8674.

ZHAO, J. Cancer stem cells and chemoresistance: The smartest survives the raid. **Pharmacol Ther**, v. 160, p. 145-58, Apr 2016. ISSN 0163-7258.